

Supporting Information

Site-Selective Halogenation on *meso*-Mesityl Substituents of 10,20-Dimesityl-5,15- Diazaporphyrins with An AuX₃/AgOTf Combination

Jean-François Longevial, Kazuya Miyagawa, and Hiroshi
Shinokubo*

*Department of Molecular and Macromolecular Chemistry, Graduate School of Engineering,
Nagoya University, Chikusa-ku, Nagoya, Aichi 464-8603, Japan.*

E-mail: hshino@chembio.nagoya-u.ac.jp

Table of Contents

Instrumentation and Materials	S2
Synthetic Procedure and Characterizations of Compounds	S3
NMR, MS, and UV-Vis Spectra of Compounds	S12
X-ray Diffraction Analysis	S48
Electrochemical Analysis	S49
Theoretical Calculations	S51
References	S52

Instrumentation and Materials

^1H NMR (500 MHz), ^{13}C NMR (126 MHz), and ^{19}F NMR (470 MHz) spectra were recorded on a Bruker AVANCE III HD spectrometer. Chemical shifts were reported as the delta scale in ppm relative to CDCl_3 ($\delta = 7.26$ ppm) for ^1H NMR, CDCl_3 ($\delta = 77.16$ ppm) for ^{13}C NMR, and hexafluorobenzene ($\delta = -162.9$ ppm) for ^{19}F NMR. UV/vis absorption spectra were recorded on a Shimadzu UV-2550 spectrometer. Emission spectra were recorded using a JASCO FP-6500 spectrometer, and absolute fluorescence quantum yields were measured by the photon-counting method using an integration sphere. High-resolution electrospray ionization time-of-flight (APCI-TOF) mass spectra were taken on a Bruker micrOTOF instrument. The progress of the reaction was monitored by MALDI-TOF-MS analysis on a Bruker autoflex TOF. 10,20-Dimesityl-5,15-diazaporphyrin **1H** and its nickel(II) complex **1Ni** were synthesized according to the literature.¹ Unless otherwise noted, materials obtained from commercial suppliers were used without further purification.

Synthetic Procedure and Characterization of Compounds

Chlorination on the mesityl groups of diazaporphyrins 1H. A grinded powder of gold(III) trichloride (80 mg, 0.18 mmol, 1 equiv) and silver(I) triflate (280 mg, 1.1 mmol, 6 equiv) was added to a solution of 10,20-dimesityl-5,15-diazaporphyrin **1H** (100 mg, 0.18 mmol) in dichloroethane (12 mL). The color of the solution changed from purple to deep blue. The resulting mixture was heated to 85 °C. After stirring for 1 h, gold(III) trichloride (160 mg, 0.36 mmol, 2 equiv) was added. Again, another portion of gold(III) trichloride (160 mg, 0.36 mmol, 2 equiv) was added after 1 h. Then, a saturated solution of NaHCO₃ (12 mL) was added and the mixture was stirred for 15 min. Then, the organic layer was washed with water (3 × 10 mL), dried over Na₂SO₄, and evaporated to dryness. The crude product was purified by silica gel column chromatography (CH₂Cl₂ as an eluent) to afford 10-(3-chloro-2,4,6-trimethylphenyl)-20-mesityl-5,15-diazaporphyrin **2H-Cl** in 12 % yield (12.6 mg) and 10,20-di(3-chloro-2,4,6-trimethylphenyl)-5,15-diazaporphyrin **3H-Cl** in 40% yield (45 mg), respectively.

Bromination on the mesityl groups of diazaporphyrins 1H. A grinded powder of gold(III) tribromide (238 mg, 0.55 mmol, 3 equiv) and silver(I) triflate (280 mg, 1.1 mmol, 6 equiv) was added to a solution of 10,20-dimesityl-5,15-diazaporphyrin **1H** (100 mg, 0.18 mmol) in dichloroethane (12 mL). The color of the solution changed from purple to deep blue. The resulting mixture was heated to 85 °C for 3 h. Afterwards, a saturated solution of

NaHCO₃ (12 mL) was added and the mixture was stirred for 15 min. Then, the organic layer was washed with water (3 × 10 mL), dried over Na₂SO₄, and evaporated to dryness. The crude product was purified by silica gel column chromatography (CH₂Cl₂ as an eluent) to afford 10-(3-bromo-2,4,6-trimethylphenyl)-20-mesityl-5,15-diazaporphyrin **2H-Br** in 7 % yield (8 mg) and 10,20-di(3-bromo-2,4,6-trimethylphenyl)-5,15-diazaporphyrin **3H-Br** in 60% yield (77 mg), respectively.

10-(3-Chloro-2,4,6-trimethylphenyl)-20-mesityl-5,15-diazaporphyrin 2H-Cl. ¹H NMR (500 MHz, CDCl₃, 298 K): δ 9.28 (d, 2H, ³J_{H-H} = 5.0 Hz, H_{β-pyrr}), 9.27 (d, 2H, ³J_{H-H} = 5.0 Hz, H_{β-pyrr}), 8.87 (d, 2H, ³J_{H-H} = 5.0 Hz, H_{β-pyrr}), 8.83 (d, 2H, ³J_{H-H} = 5.0 Hz, H_{β-pyrr}), 7.39 (s, 1H, H_{Ar-meso}), 7.31 (s, 2H, H_{Ar-meso}), 2.72 (s, 3H, H_{p-Me}), 2.64 (s, 3H, H_{p-Me}), 1.95 (s, 3H, H_{o-Me}), 1.85 (s, 6H, H_{o-Me}), 1.80 (s, 3H, H_{o-Me}), -2.56 (bs, 2H, H_{NH}) ppm. ¹³C NMR (125 MHz, CDCl₃, 298 K): δ 139.4, 139.4, 138.8, 137.8, 137.6, 137.2, 135.6, 133.4, 133.0, 132.8, 129.6, 128.3, 121.5, 120.6, 21.9, 21.6, 21.4, 20.1 ppm. MS (APCI-TOF): calcd for [M+H]⁺ C₃₆H₃₂ClN₆: 583.2371. Found *m/z* = 583.2387. UV-Vis (CH₂Cl₂) λ_{max} (ε): 393 (100120), 485 (3340), 508 (5560), 543 (24100), 579 (6720), 628 (32900).

10,20-Di(3-chloro-2,4,6-trimethylphenyl)-5,15-diazaporphyrin 3H-Cl. ¹H NMR (500 MHz, CDCl₃, 298 K): δ 9.29 (d, 4H, ³J_{H-H} = 5.0 Hz, H_{β-pyrr}), 8.84 (d, 4H, ³J_{H-H} = 5.0 Hz, H_{β-pyrr}), 7.40 (s, 2H, H_{Ar-meso}), 2.72 (s, 6H, H_{p-Me}), 1.95 (s, 6H, H_{o-Me}), 1.80 (s, 6H, H_{o-Me}), -2.56 (bs, 2H, H_{NH}) ppm. ¹³C NMR (125 MHz, CDCl₃, 298 K): δ 137.8, 137.5, 137.2, 133.6, 132.8,

132.7, 132.2, 129.6, 120.7, 21.6, 21.4, 20.1 ppm. MS (APCI-TOF): calcd for $[M+H]^+$ $C_{36}H_{31}Cl_2N_6$: 617.1981. Found $m/z = 617.1968$. UV-Vis (CH_2Cl_2) λ_{max} (ϵ): 393 (88860), 485 (2980), 508 (4830), 543 (21550), 578 (5150), 628 (29760). Fluorescence (CH_2Cl_2 , $\lambda_{ex} = 550$ nm): $\lambda_{em} = 635.5$ and 695.2 nm, $\Phi_f = 0.009$.

10-(3-Bromo-2,4,6-trimethylphenyl)-20-mesityl-5,15-diazaporphyrin 2H-Br. 1H NMR (500 MHz, $CDCl_3$, 298 K): δ 9.28 (d, 2H, $^3J_{H-H} = 5.0$ Hz, $H_{\beta-pyrr}$), 9.27 (d, 2H, $^3J_{H-H} = 5.0$ Hz, $H_{\beta-pyrr}$), 8.87 (d, 2H, $^3J_{H-H} = 5.0$ Hz, $H_{\beta-pyrr}$), 8.83 (d, 2H, $^3J_{H-H} = 5.0$ Hz, $H_{\beta-pyrr}$), 7.40 (s, 1H, $H_{Ar-meso}$), 7.32 (s, 2H, $H_{Ar-meso}$), 2.76 (s, 3H, H_{p-Me}), 2.64 (s, 3H, H_{p-Me}), 2.00 (s, 3H, H_{o-Me}), 1.85 (s, 6H, H_{o-Me}), 1.78 (s, 3H, H_{o-Me}), -2.56 (bs, 2H, H_{NH}) ppm. ^{13}C NMR (125 MHz, $CDCl_3$, 298 K): δ 154.1, 148.1, 139.6, 139.4, 139.4, 139.3, 138.8, 138.5, 137.5, 135.6, 133.4, 133.0, 132.6, 131.0, 129.5, 129.0, 128.3, 125.8, 121.5, 120.8, 24.6, 23.4, 21.9, 21.6, 21.6 ppm. APCI-TOF-MS: calcd for $[M+H]^+$ $C_{36}H_{32}BrN_6$: 627.1866. Found $m/z = 627.1874$. UV-Vis (CH_2Cl_2) λ_{max} (ϵ) 394 (109230), 486 (3700), 508 (6030), 543 (26070), 578 (6240), 628 (35900).

10,20-Di(3-bromo-2,4,6-trimethylphenyl)-5,15-diazaporphyrin 3H-Br. 1H NMR (500 MHz, $CDCl_3$, 298 K): δ 9.29 (d, 4H, $^3J_{H-H} = 5.0$ Hz, $H_{\beta-pyrr}$), 8.84 (d, 4H, $^3J_{H-H} = 5.0$ Hz, $H_{\beta-pyrr}$), 7.40 (s, 2H, $H_{Ar-meso}$), 2.76 (s, 6H, H_{p-Me}), 2.00 (s, 6H, H_{o-Me}), 1.78 (s, 6H, H_{o-Me}), -2.56 (bs, 2H, H_{NH}) ppm. ^{13}C NMR (125 MHz, $CDCl_3$, 298 K): δ 154.3, 148.3, 139.6, 139.6, 139.3, 138.5, 138.5, 137.4, 133.6, 133.6, 132.7, 132.7, 129.5, 125.8, 120.9, 24.6, 23.5, 21.7

ppm. APCI-TOF-MS: calcd for $[M+H]^+$ $C_{36}H_{31}Br_2N_6$: 705.0971. Found $m/z = 705.0974$. UV-Vis (CH_2Cl_2) λ_{max} (ϵ): 394 (103304), 486 (3420), 508 (5670), 543 (25100), 578 (5800), 628 (34750). Fluorescence (CH_2Cl_2 , $\lambda_{ex} = 550$ nm): $\lambda_{em} = 636.4$ and 695.7 nm, $\Phi_f = 0.008$.

Bromination on the core of 10,20-diphenyl-5,15-diazaporphyrin 4. A grinded powder of gold(III) tribromide (52.5 mg, 0.12 mmol, 3 equiv) and silver(I) triflate (61.6 mg, 0.24 mmol, 6 equiv) was added to a solution of 10,20-diphenyl-5,15-diazaporphyrin **4** (18.6 mg, 0.04 mmol) in dichloroethane (3.0 mL). The color of the solution changed from purple to deep blue. The resulting mixture was heated to 85 °C for 3 h. Afterwards, a saturated solution of $NaHCO_3$ (12 mL) was added and the mixture was stirred for 15 min. Then, the organic layer was washed with water (3×10 mL), dried over Na_2SO_4 , and evaporated to dryness. The crude product was purified by silica gel column chromatography (CH_2Cl_2 as an eluent) to afford 2-bromo-10,20-diphenyl-5,15-diazaporphyrin **5** in 9 % yield (2.0 mg).

3-Bromo-10,20-diphenyl-5,15-diazaporphyrin 5. 1H NMR (500 MHz, $CDCl_3$, 298 K): δ 9.38 (d, 1H, $^3J_{H-H} = 4.5$ Hz, $H_{\beta-pyrr}$), 9.30 (d, 1H, $^3J_{H-H} = 5.0$ Hz, $H_{\beta-pyrr}$), 9.09 (d, 1H, $^3J_{H-H} = 4.0$ Hz, $H_{\beta-pyrr}$), 9.05 (d, 1H, $^3J_{H-H} = 4.5$ Hz, $H_{\beta-pyrr}$), 9.02 (d, 1H, $^3J_{H-H} = 4.5$ Hz, $H_{\beta-pyrr}$), 8.91 (s, 1H, $H_{\beta-pyrr}$), 8.82 (d, 1H, $^3J_{H-H} = 4.5$ Hz, $H_{\beta-pyrr}$), 8.18–8.22 (m, 4H, H_{Ph}), 7.82–7.86 (m, 6H, H_{Ph}), –3.30 (bs, 2H, H_{NH}) ppm. ^{13}C NMR (125 MHz, $CDCl_3$, 298 K): δ 139.2, 139.1, 136.2, 135.5, 135.4, 135.0, 134.8, 131.7, 131.6, 130.9, 130.2, 128.7, 128.6, 127.5,

127.4, 126.5, 122.7, 122.5 ppm. APCI-TOF-MS: calcd for $[M]^+$ C₃₀H₁₉BrN₆: 542.0849.

Found m/z = 542.0834.

Suzuki–Miyaura coupling on the aryl substituents. In a narrow Schlenk tube, 10,20-di(3-bromo-2,4,6-trimethylphenyl)-5,15-diazaporphyrin **3H-Br** (5.2 mg, 7.36 μ mol) was charged. Then phenylboronic acid (3.6 mg, 29.5 μ mol, 4 equiv), K₃PO₄ (12.5 mg, 58.8 μ mol, 8 equiv), Pd₂(dba)₃•CHCl₃ (1 mg, 0.74 μ mol, 10 mol%), and SPhos (1 mg, 1.47 μ mol) were added, and the Schlenk tube was capped with a septum and sealed with electrical tape. The Schlenk tube was evacuated and back filled with nitrogen 3 times. Then, distilled toluene (1 mL) was added and the resulting mixture was stirred at 100 °C for 2 h and additional 12 h at 60 °C. The progress of the reaction was monitored by MALDI-TOF-MS analysis of the reaction mixture. The mixture was then cooled to room temperature, and CH₂Cl₂ (5 mL) and water (5 mL) were added. The organic layer was then washed two times with 1 M NaOH aqueous solution, dried over anhydrous Na₂SO₄, and evaporated to dryness. Finally, the residue was purified by silica-gel column chromatography (CH₂Cl₂/AcOEt = 20/1) to provide 10,20-di(3-phenyl-2,4,6-trimethylphenyl)-5,15-diazaporphyrin **8a** as a purple solid in 95% yield.

10-(3-Phenyl-2,4,6-trimethylphenyl)-20-mesityl-5,15-diazaporphyrin 7. ¹H NMR (500 MHz, CDCl₃, 298 K): δ 9.30 (d, 2H, ³J_{H-H} = 5.0 Hz, H _{β -pyrr}), 9.27 (d, 2H, ³J_{H-H} = 5.0 Hz,

$H_{\beta\text{-pyrr}}$), 8.96 (d, 2H, $^3J_{\text{H-H}} = 5.0$ Hz, $H_{\beta\text{-pyrr}}$), 8.86 (d, 2H, $^3J_{\text{H-H}} = 5.0$ Hz, $H_{\beta\text{-pyrr}}$), 7.51–7.35 (m, 5H, H_{Ph}), 7.31, (bs, 3H, $H_{\text{Ar-meso}}$), 2.64 (s, 3H, H_{Me}), 2.35 (s, 3H, H_{Me}), 1.87–1.83 (m, 9H, H_{Me}), 1.54 (s, 3H, H_{Me}), –2.53 (bs, 2H, H_{NH}) ppm. ^{13}C NMR (125 MHz, CDCl_3 , 298 K): δ 154.0, 147.9, 141.4, 139.9, 139.4, 139.4, 138.7, 138.4, 137.6, 136.9, 136.3, 135.7, 133.2, 132.9, 129.7, 128.7, 128.2, 126.9, 121.8, 121.3, 21.9, 21.9, 21.8, 21.6 ppm. APCI-TOF-MS: calcd for $[\text{M}+\text{H}]^+$ $\text{C}_{42}\text{H}_{37}\text{N}_6$: 625.3074. Found $m/z = 625.3091$. UV-Vis (CH_2Cl_2) λ_{max} (ϵ): 395 (81830), 485 (2730), 508 (4470), 543 (19230), 578 (4620), 629 (26030).

10,20-Di(3-phenyl-2,4,6-trimethylphenyl)-5,15-diazaporphyrin 8a. ^1H NMR (500 MHz, CDCl_3 , 298 K): δ 9.30 (d, 4H, $^3J_{\text{H-H}} = 5.0$ Hz, $H_{\beta\text{-pyrr}}$), 8.96 (d, 4H, $^3J_{\text{H-H}} = 5.0$ Hz, $H_{\beta\text{-pyrr}}$), 7.51–7.34 (m, 12H, H_{Ph} and $H_{\text{Ar-meso}}$), 2.35 (s, 6H, H_{Me}), 1.88 (s, 3H, H_{Me}), 1.85 (s, 3H, H_{Me}), 1.56 (s, 3H, H_{Me}), 1.53 (s, 3H, H_{Me}), –2.52 (bs, 2H, H_{NH}) ppm. ^{13}C NMR (125 MHz, CDCl_3 , 298 K): δ 154.2, 148.3, 141.4, 139.9, 138.4, 138.4, 137.6, 137.5, 136.9, 136.3, 133.3, 132.9, 129.7, 128.7, 126.9, 121.8, 21.9, 21.9, 21.4, 20.5, 20.4 ppm. APCI-TOF-MS: calcd for $[\text{M}+\text{H}]^+$ $\text{C}_{48}\text{H}_{41}\text{N}_6$: 701.3387. Found $m/z = 701.3352$. UV-Vis (CH_2Cl_2) λ_{max} (ϵ): 395 (81900), 486 (2680), 508 (4430), 544 (19560), 578 (4640), 629 (26830). Fluorescence (CH_2Cl_2 , $\lambda_{\text{ex}} = 550$ nm): $\lambda_{\text{em}} = 636.9$ and 696.1 nm, $\Phi_{\text{f}} = 0.04$.

10,20-Di(2,4,6-trimethyl-3-(1-naphthyl)phenyl)-5,15-diazaporphyrin 8b. ^1H NMR (500 MHz, CDCl_3 , 298 K): δ 9.34 (d, 2H, $^3J_{\text{H-H}} = 5.0$ Hz, $H_{\beta\text{-pyrr}}$), 9.31 (d, 2H, $^3J_{\text{H-H}} = 5.0$ Hz,

H $_{\beta}$ -pyrr), 9.03 (d, 2H, $^3J_{H-H} = 5.0$ Hz, H $_{\beta}$ -pyrr), 9.02 (d, 2H, $^3J_{H-H} = 5.0$ Hz, H $_{\beta}$ -pyrr), 7.96–7.41 (m, 16H, H $_{Naphthalene}$; H $_{Ar-meso}$), 2.23 (s, 6H, H $_{Me}$), 1.92 (2s, 6H, H $_{Me}$), 1.44 (2s, 6H, H $_{Me}$), –2.52 (bs, 2H, H $_{NH}$) ppm. ^{13}C NMR (125 MHz, CDCl $_3$, 298 K): δ 154.5, 148.0, 143.5, 138.8, 138.8, 138.6, 138.5, 138.1, 137.6, 136.4, 134.1, 133.3, 132.9, 132.3, 132.3, 131.0, 129.1, 129.0, 128.9, 128.7, 128.5, 127.6, 127.3, 126.6, 126.1, 126.0, 125.4, 125.4, 121.7, 22.0, 22.0, 21.9, 20.9, 20.9 ppm. APCI-TOF-MS: calcd for [M+H] $^+$ C $_{56}$ H $_{45}$ N $_6$: 801.3700. Found m/z = 801.3669. UV-Vis (CH $_2$ Cl $_2$) λ_{max} (ϵ): 284 (20500), 294 (19800), 396 (92760), 486 (3000), 508 (4900), 544 (22000), 578 (5200), 629 (30400). Fluorescence (CH $_2$ Cl $_2$, $\lambda_{ex} = 550$ nm): $\lambda_{em} = 636.5$ and 696.1 nm, $\Phi_f = 0.03$.

10,20-Di(3-(4-trifluoromethyl)phenyl)-2,4,6-trimethylphenyl)-5,15-diazaporphyrin

8c. 1H NMR (500 MHz, CDCl $_3$, 298 K): δ 9.24 (d, 4H, $^3J_{H-H} = 5.0$ Hz, H $_{\beta}$ -pyrr), 9.87 (d, 4H, $^3J_{H-H} = 5.0$ Hz, H $_{\beta}$ -pyrr), 7.70–7.68 (m, 4H, H $_{Ph}$), 7.51–7.49 (m, 4H, H $_{Ph}$), 7.37, (s, 2H, H $_{Ar-meso}$), 2.26 (s, 6H, H $_{Me}$), 1.81 (2s, 6H, H $_{Me}$), 1.44 (2s, 6H, H $_{Me}$), –2.60 (bs, 2H, H $_{NH}$) ppm. ^{19}F NMR (470 MHz, CDCl $_3$, 298 K): δ –62.38 (s, CF $_3$) ppm. ^{13}C NMR (125 MHz, CDCl $_3$, 298K): 154.1, 148.3, 145.2, 139.1, 138.6, 137.2, 137.2, 136.7, 136.6, 133.4, 132.8, 130.2, 129.4 (q, $J = 32.4$ MHz), 129.0, 125.8, 124.4 (q, $J = 272.7$ MHz), 121.4, 21.9, 21.9, 21.4, 20.4, 20.4 ppm. APCI-TOF-MS: calcd for [M+H] $^+$ C $_{50}$ H $_{39}$ F $_6$ N $_6$: 837.3134. Found m/z = 837.3106. UV-Vis (CH $_2$ Cl $_2$) λ_{max} (ϵ): 395 (94676), 486 (3000), 508 (5040), 543 (22480), 578 (5210), 629 (30730). Fluorescence (CH $_2$ Cl $_2$, $\lambda_{ex} = 550$ nm): $\lambda_{em} = 634.9$ and 695.7 nm, $\Phi_f =$

0.05.

10,20-Di(3-(4-methoxy)phenyl-2,4,6-trimethylphenyl)-5,15-diazaporphyrin 8d. ¹H

NMR (500 MHz, CDCl₃, 298 K): δ 9.30 (d, 4H, ³J_{H-H} = 5.0 Hz, H _{β -pyrr}), 8.95 (d, 4H, ³J_{H-H} = 5.0 Hz, H _{β -pyrr}), 7.41 (s, 1H, H_{Ar-meso}), 7.40 (s, 1H, H_{Ar-meso}), 7.35–7.33 (m, 4H, H_{Ph}), 7.05–7.02 (m, 4H, H_{Ph}), 3.86 (2s, 6H, H_{OMe}), 2.36 (s, 6H, H_{Me}), 1.88 (2s, 6H, H_{Me}), 1.56 (2s, 6H, H_{Me}), –2.52 (bs, 2H, H_{NH}) ppm. ¹³C NMR (125 MHz, CDCl₃, 298 K): δ 158.4, 153.9, 148.2, 139.4, 138.1, 138.1, 137.9, 137.9, 136.1, 133.4, 133.1, 132.8, 130.6, 128.5, 121.8, 114.0, 21.7, 21.7, 21.4, 20.4, 20.4 ppm. APCI-TOF-MS: calcd for [M+H]⁺ C₅₀H₄₅N₆O₂: 761.3598. Found m/z = 761.3562. UV-Vis (CH₂Cl₂) λ_{\max} (ϵ): 284 (20500), 294 (19800), 396 (92760), 486 (3000), 508(4900), 544 (22000), 578 (5200), 629 (30400). Fluorescence (CH₂Cl₂, λ_{ex} = 550 nm): λ_{em} = 637.1 and 696.3 nm, Φ_{f} = 0.03.

Synthesis of gold complexes 9 and 10. To a solution of **1H** (8 mg, 14.5 μ mol, 1 equiv) in dichloroethane (12 mL) at room temperature under open air, gold(III) trichloride (10 mg, 44 μ mol, 3 equiv) was added. The color of the solution changed from purple to deep blue within a few seconds. Afterwards, the reaction mixture was stirred at 85 °C for 3 h. Then, the solvent was removed under reduced pressure and the crude product was directly purified by silica gel column chromatography (CH₂Cl₂). The less polar green product (first fraction) consisted of bisgold complex **10** (25% yield). The second fraction (grey color) consisted of

the monogold complex **9** (32% yield).

Gold Complex 9. ^1H NMR (500 MHz, CDCl_3 , 298 K): δ 9.79 (d, 2H, $^3J_{\text{H-H}} = 5.0$ Hz, $\text{H}_{\beta\text{-pyrr}}$), 9.26 (d, 2H, $^3J_{\text{H-H}} = 5.0$ Hz, $\text{H}_{\beta\text{-pyrr}}$), 8.93 (d, 2H, $^3J_{\text{H-H}} = 5.0$ Hz, $\text{H}_{\beta\text{-pyrr}}$), 8.78 (d, 2H, $^3J_{\text{H-H}} = 5.0$ Hz, $\text{H}_{\beta\text{-pyrr}}$), 7.33 (s, 4H, $\text{H}_{\text{Ar-meso}}$), 2.65 (s, 6H, $\text{H}_{p\text{-Me}}$), 1.84 (s, 12H, $\text{H}_{o\text{-Me}}$), -1.92 (bs, 2H, H_{NH}) ppm. ^{13}C NMR (125 MHz, CDCl_3 , 298 K): 139.7, 139.1, 137.4, 136.2, 135.2, 135.1, 134.4, 137.7, 131.0, 129.9, 128.6, 126.7, 125.6, 21.9, 21.6 ppm. MALDI-TOF-MS: calcd for $[\text{M}+\text{H}]^+$ $\text{C}_{36}\text{H}_{33}\text{AuCl}_3\text{N}_6$: 851.1420. Found $m/z = 851.150$. UV-Vis (CH_2Cl_2) λ_{max} (ϵ): 390 (80260), 566 (12960), 592 (8650), 641 (40810).

Gold Complex 10. ^1H NMR (500 MHz, CDCl_3 , 298 K): δ 9.86 (d, 4H, $^3J_{\text{H-H}} = 5.0$ Hz, $\text{H}_{\beta\text{-pyrr}}$), 8.92 (d, 4H, $^3J_{\text{H-H}} = 5.0$ Hz, $\text{H}_{\beta\text{-pyrr}}$), 7.37 (s, 4H, $\text{H}_{\text{Ar-meso}}$), 2.66 (s, 6H, $\text{H}_{p\text{-Me}}$), 1.85 (s, 12H, $\text{H}_{o\text{-Me}}$), -1.67 (bs, 2H, H_{NH}) ppm. ^{13}C NMR (125 MHz, CDCl_3 , 298 K): 140.8, 139.0, 136.2, 133.5 (2C), 133.3, 130.0, 129.0, 128.6, 22.1, 21.7 ppm. MALDI-TOF-MS: calcd for $[\text{M}+\text{H}]^+$ $\text{C}_{36}\text{H}_{32}\text{Au}_2\text{Cl}_6\text{N}_6$: 1153.0151. Found $m/z = 1153.014$. UV-Vis (CH_2Cl_2) λ_{max} (ϵ): 390 (116890), 581 (18950), 608 (11200), 660 (40800).

NMR, MS, and UV-Vis Spectra of Compounds

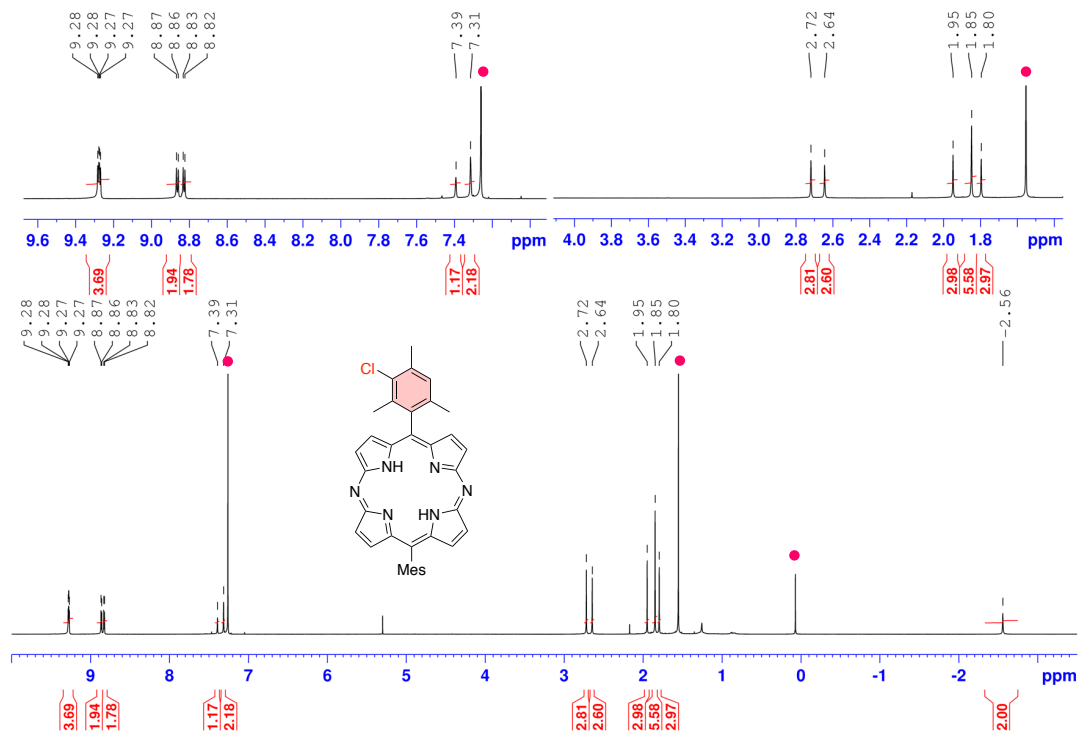


Figure S1. ^1H NMR spectrum of **2H-Cl** in CDCl_3 .

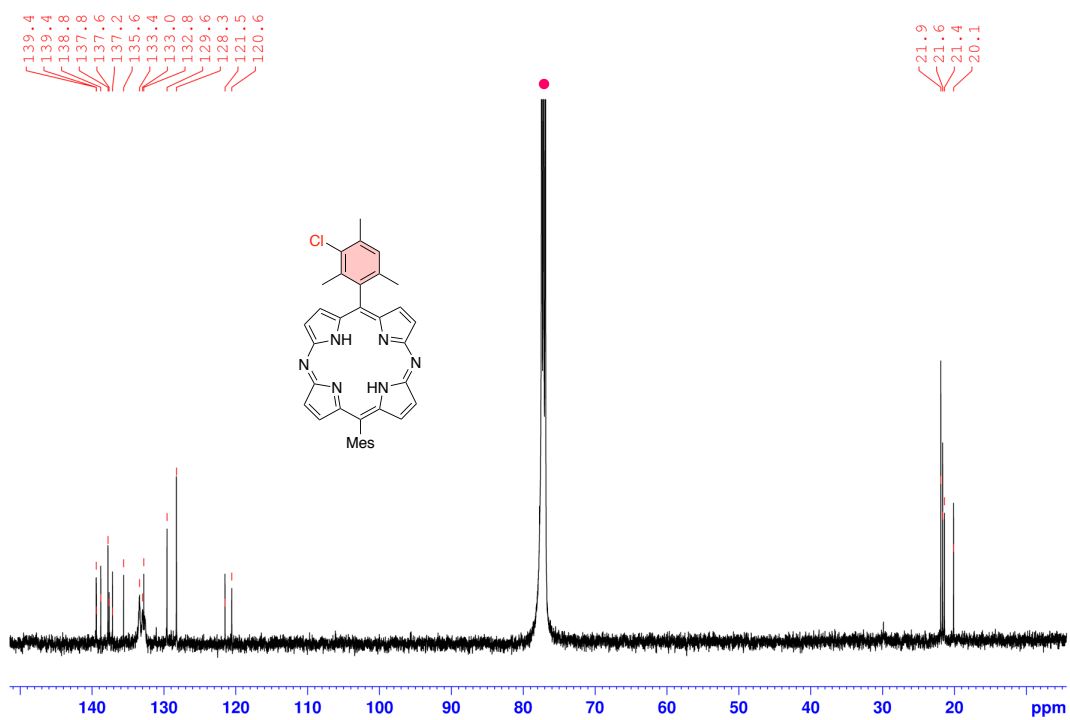


Figure S2. $^{13}\text{C}\{^1\text{H}\}$ NMR spectrum of **2H-Cl** in CDCl_3 .

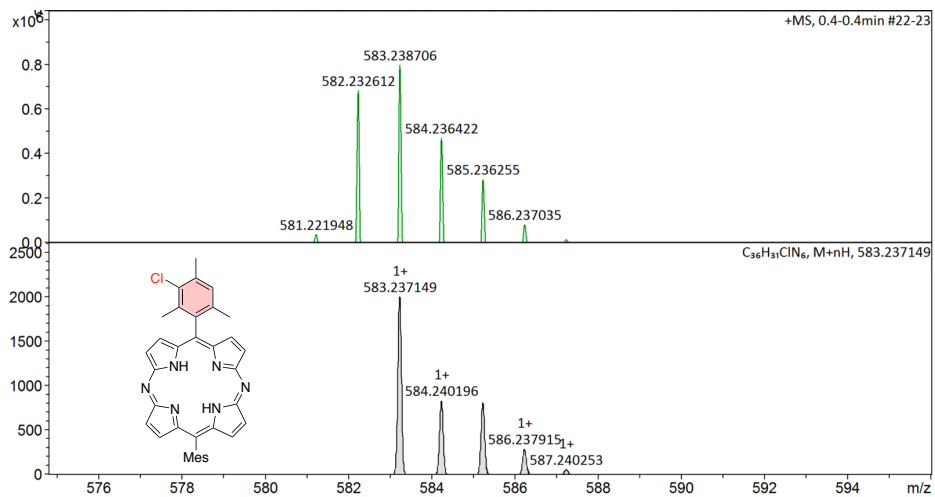


Figure S3. HR-MS spectrum of 2H-Cl.

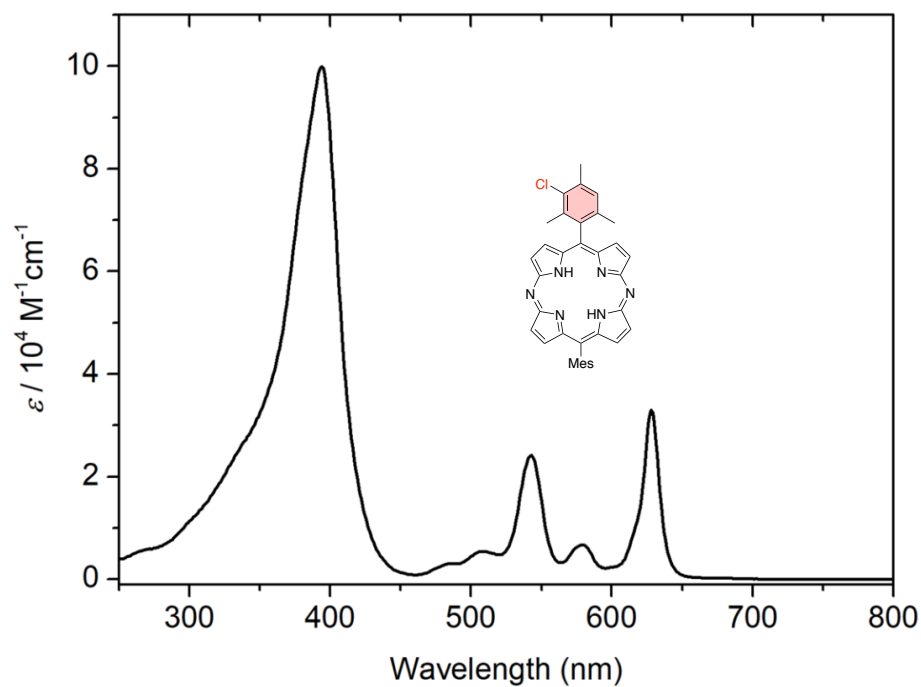


Figure S4. UV-Vis spectrum of 2H-Cl in CH₂Cl₂.

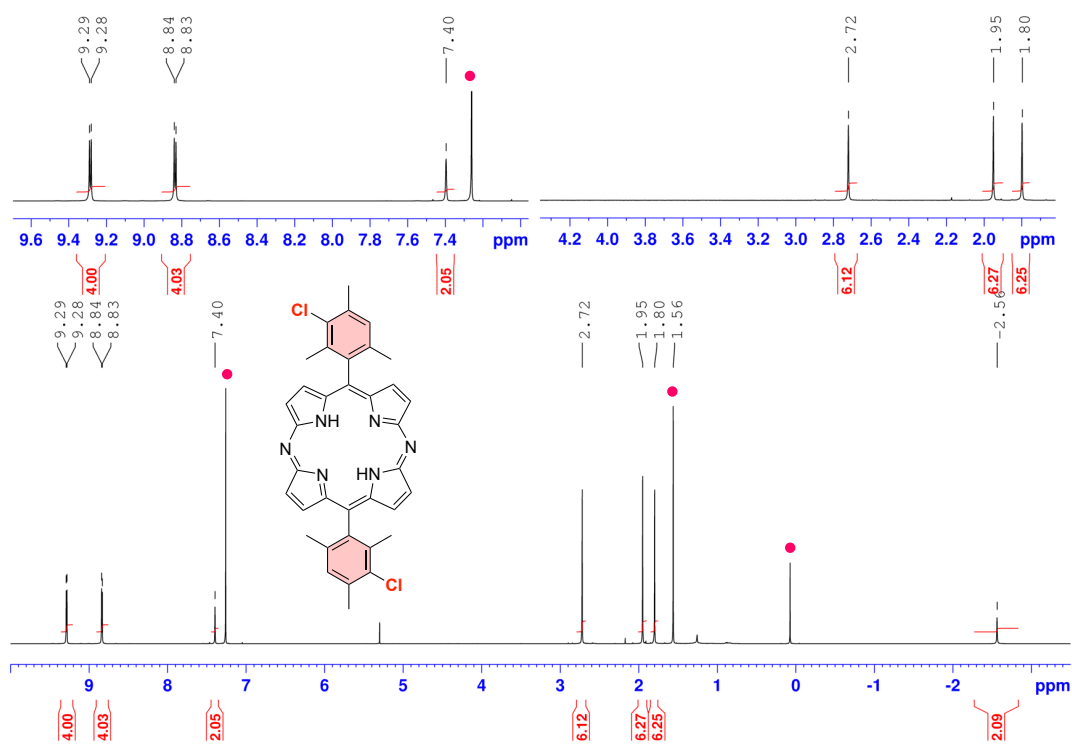


Figure S5. ^1H NMR spectrum of 3H-Cl in CDCl_3 .

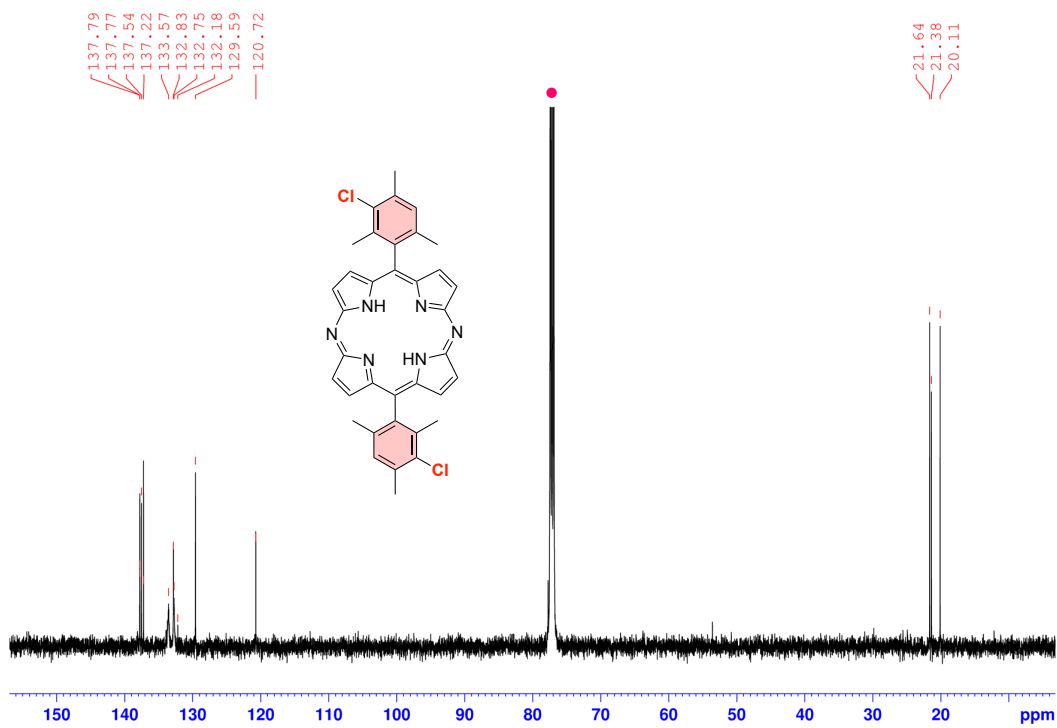


Figure S6. $^{13}\text{C}\{^1\text{H}\}$ NMR spectrum of 3H-Cl in CDCl_3 .

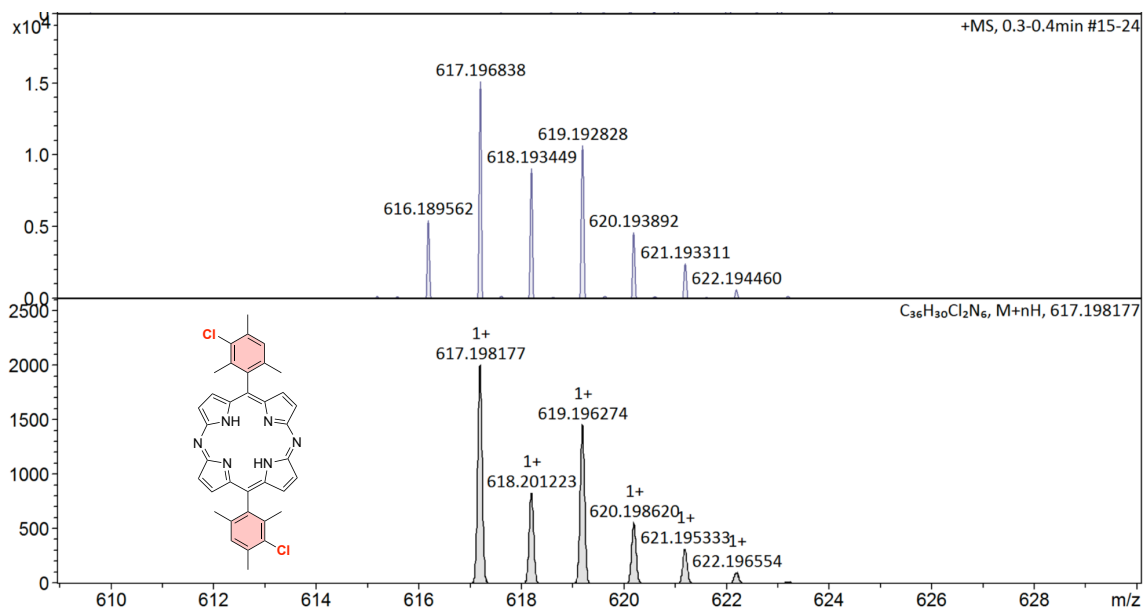


Figure S7. APCI-TOF-MS spectrum of **3H-Cl**.

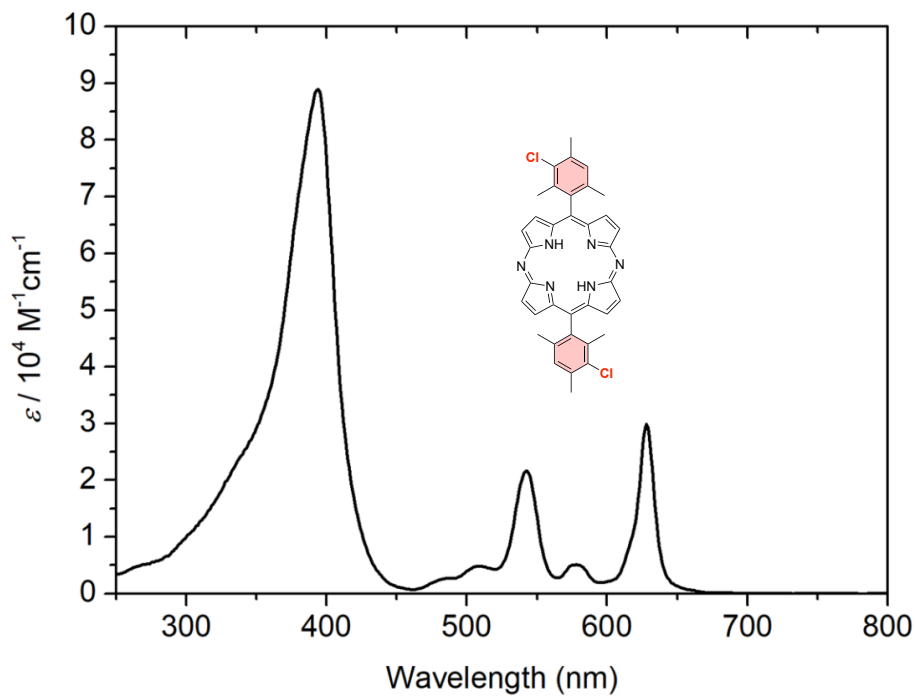


Figure S8. UV-Vis spectrum of **3H-Cl** in CH_2Cl_2 .

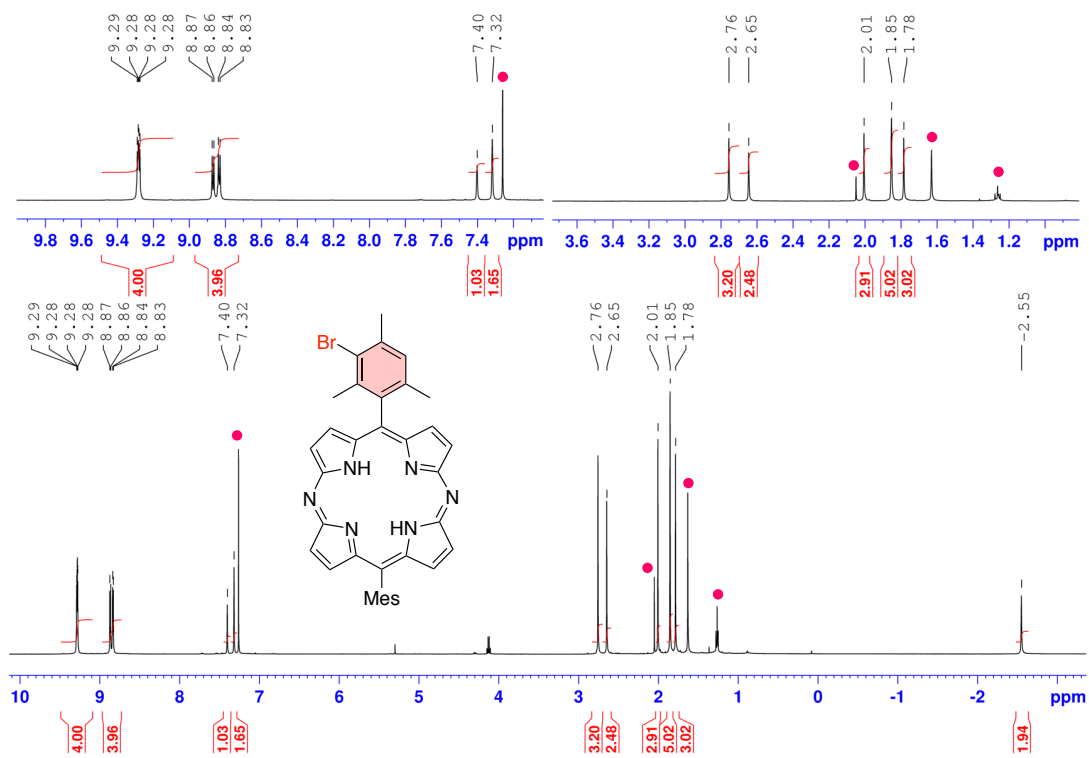


Figure S9. ^1H NMR spectrum of **2H-Br** in CDCl_3 .

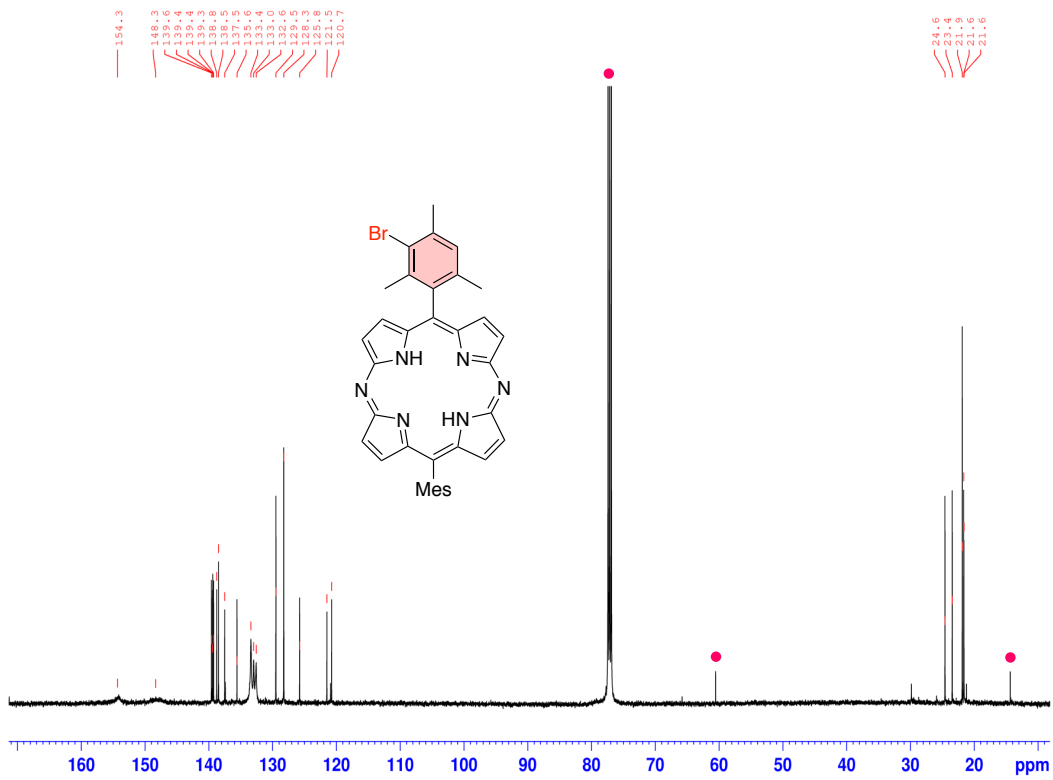


Figure S10. $^{13}\text{C}\{^1\text{H}\}$ NMR spectrum of **2H-Br** in CDCl_3 .

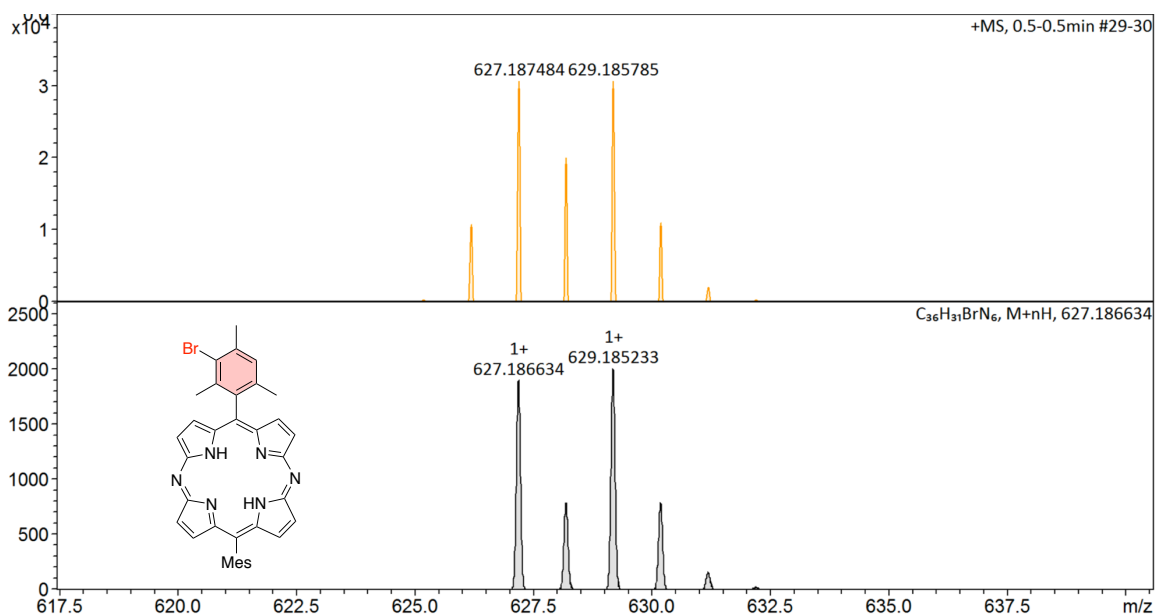


Figure S11. APCI-TOF-MS spectrum of **2H-Br**.

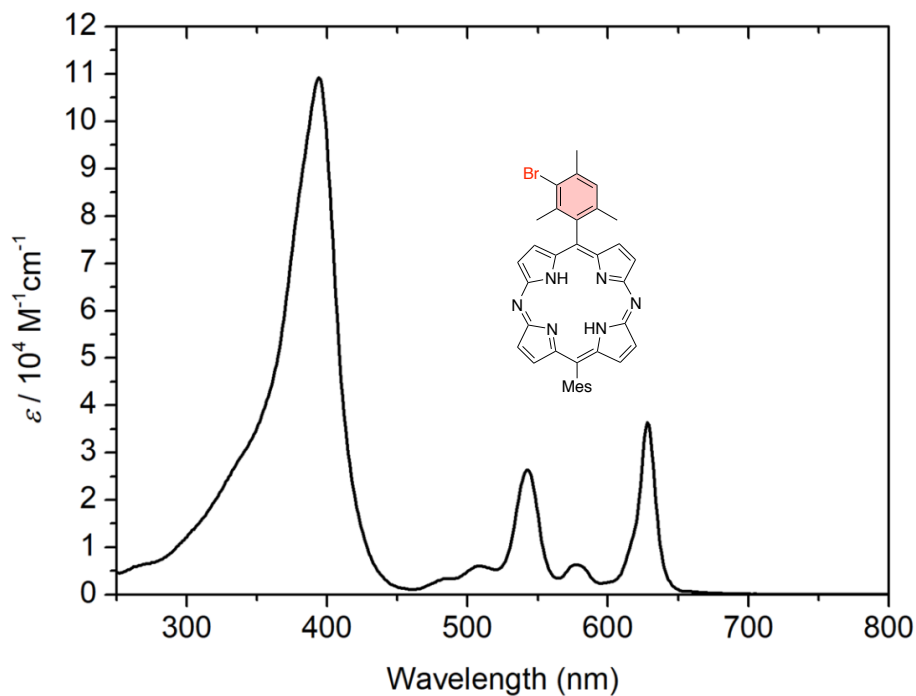


Figure S12. UV-Vis spectrum of **2H-Br** in CH_2Cl_2 .

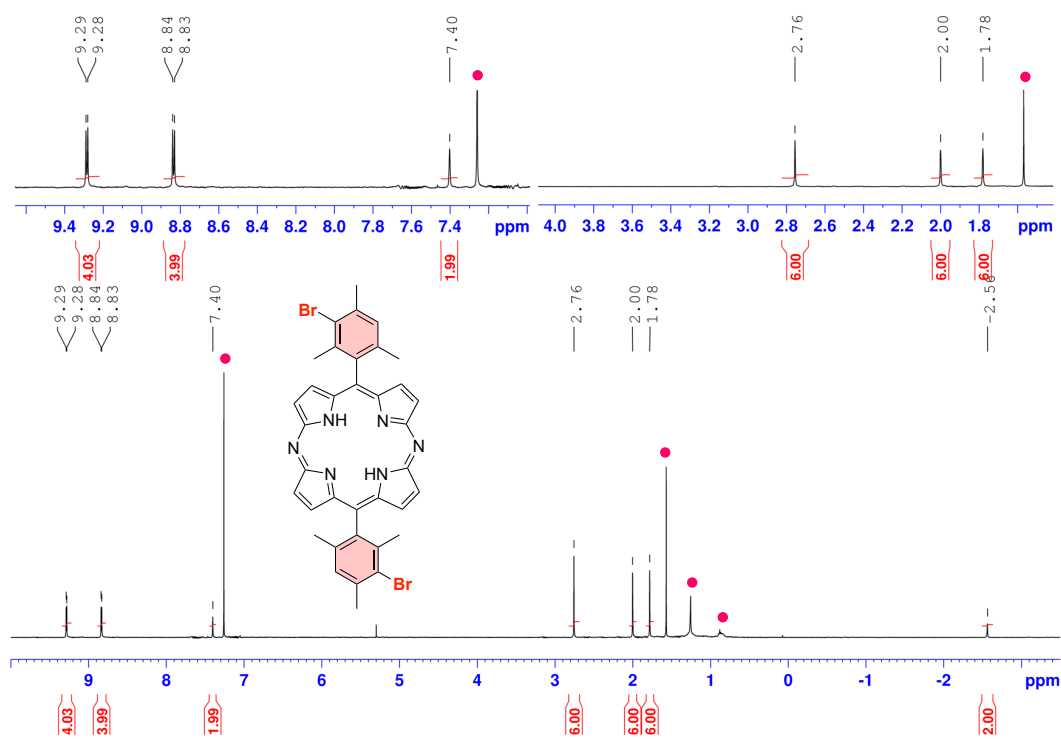


Figure S13. ^1H NMR spectrum of **3H-Br** in CDCl_3 .

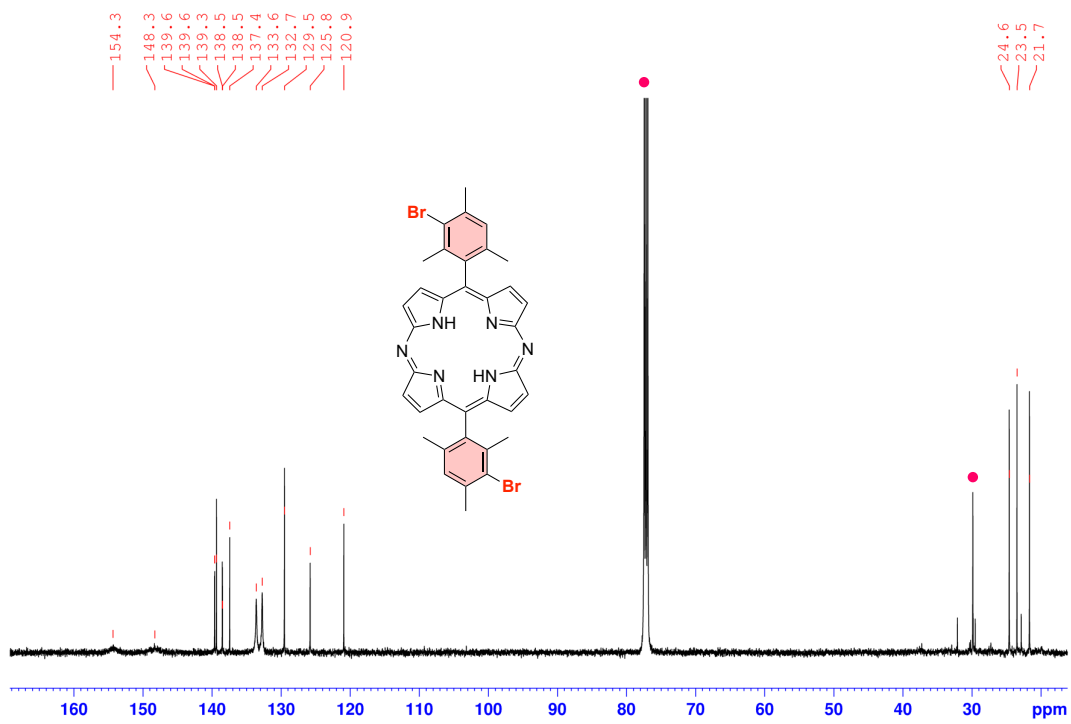


Figure S14. $^{13}\text{C}\{^1\text{H}\}$ NMR spectrum of 3H-Br in CDCl_3 .

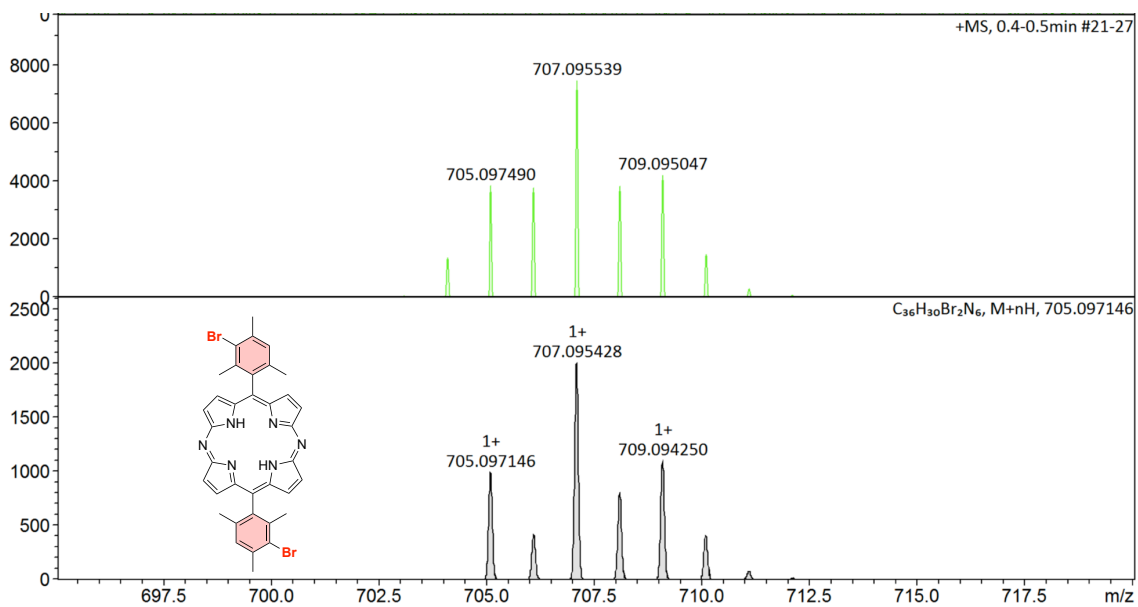


Figure S15. APCI-TOF-MS spectrum of **3H-Br**.

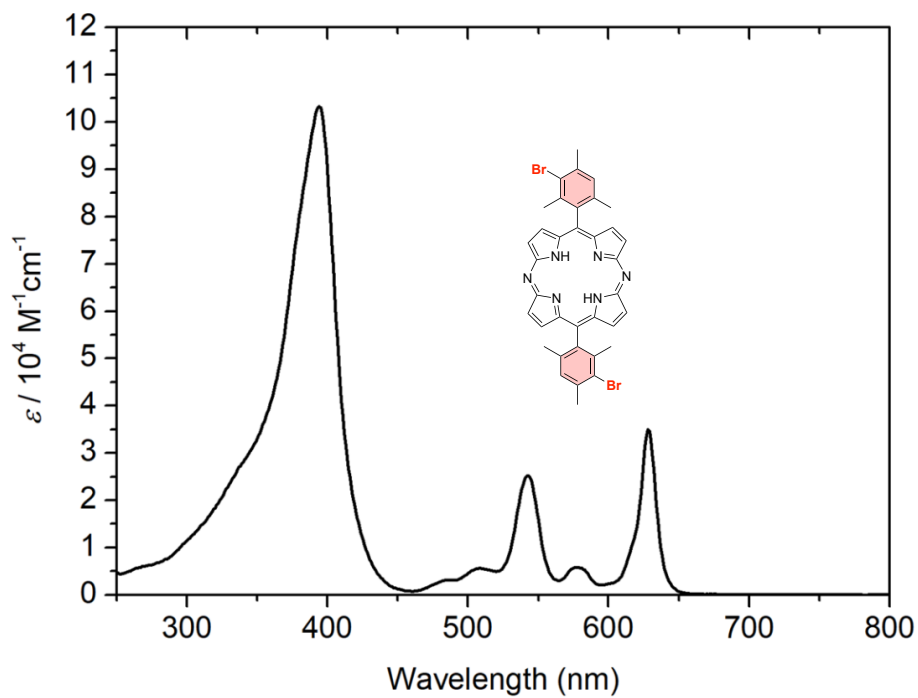


Figure S16. UV-Vis spectrum of **3H-Br** in CH_2Cl_2 .

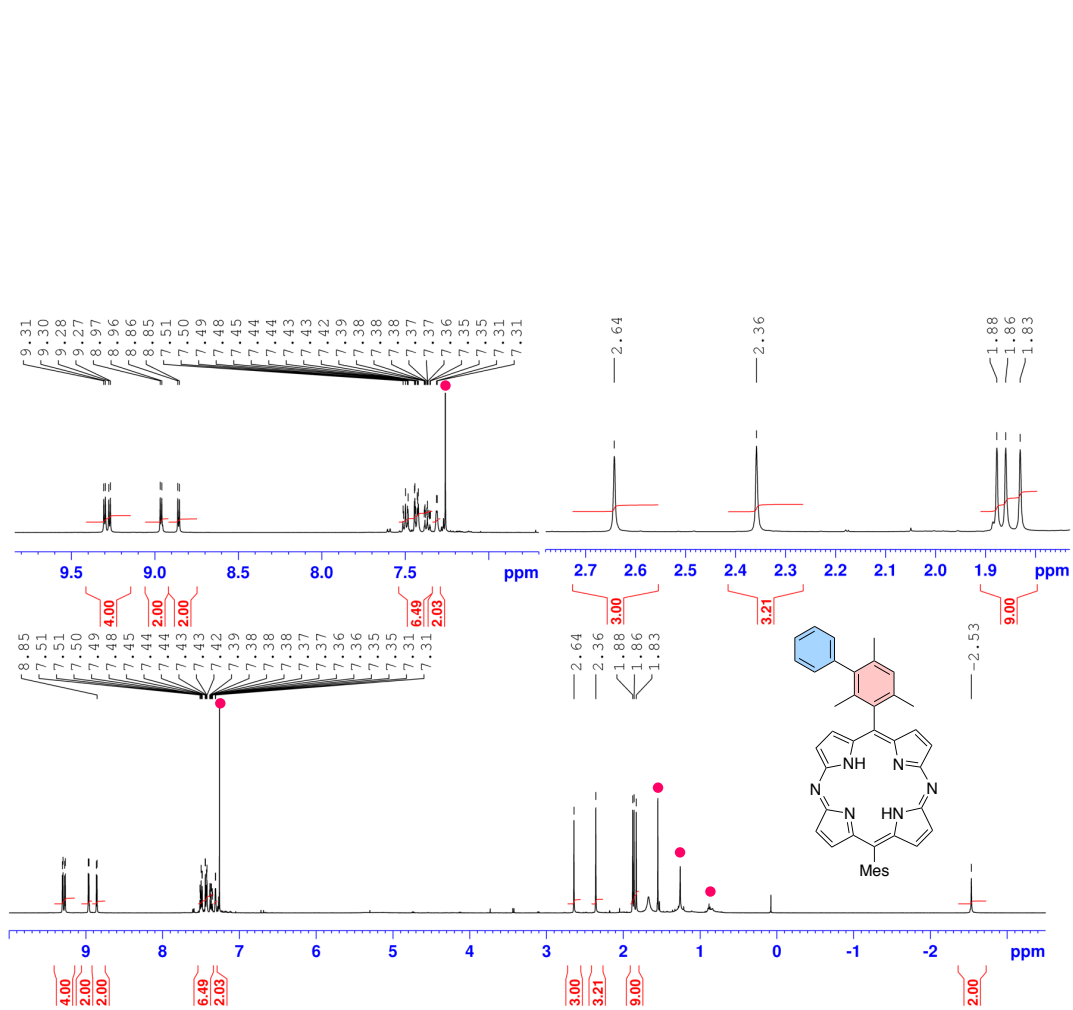


Figure S17. ^1H NMR spectrum of **7** in CDCl_3 .

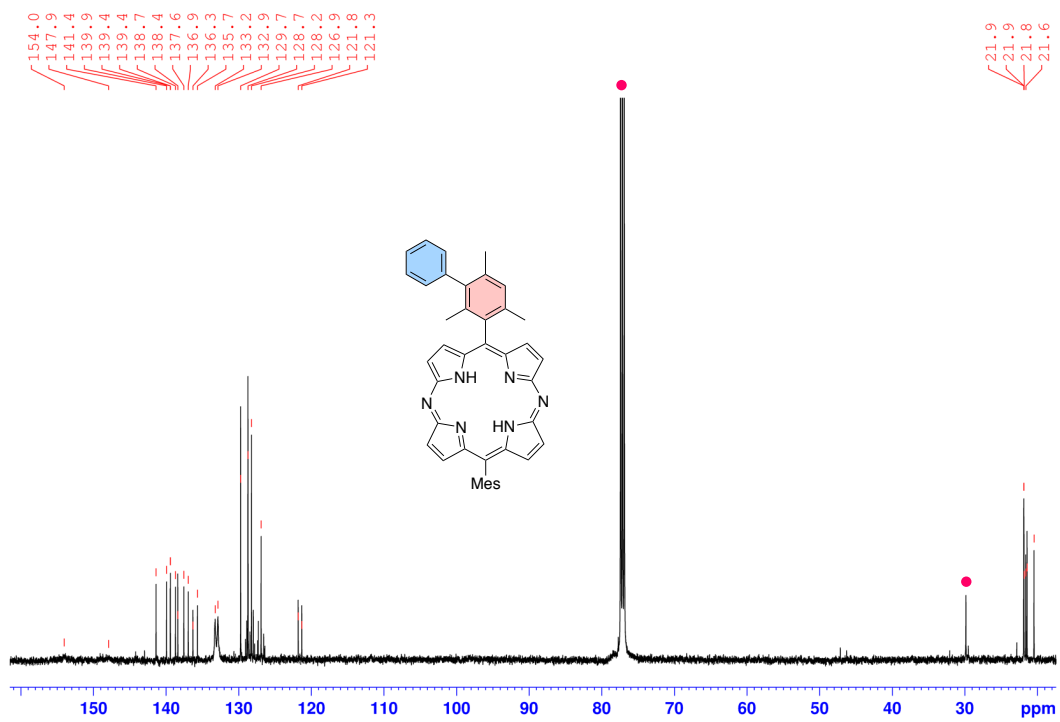


Figure S18. $^{13}\text{C}\{^1\text{H}\}$ NMR spectrum of **7** in CDCl_3 .

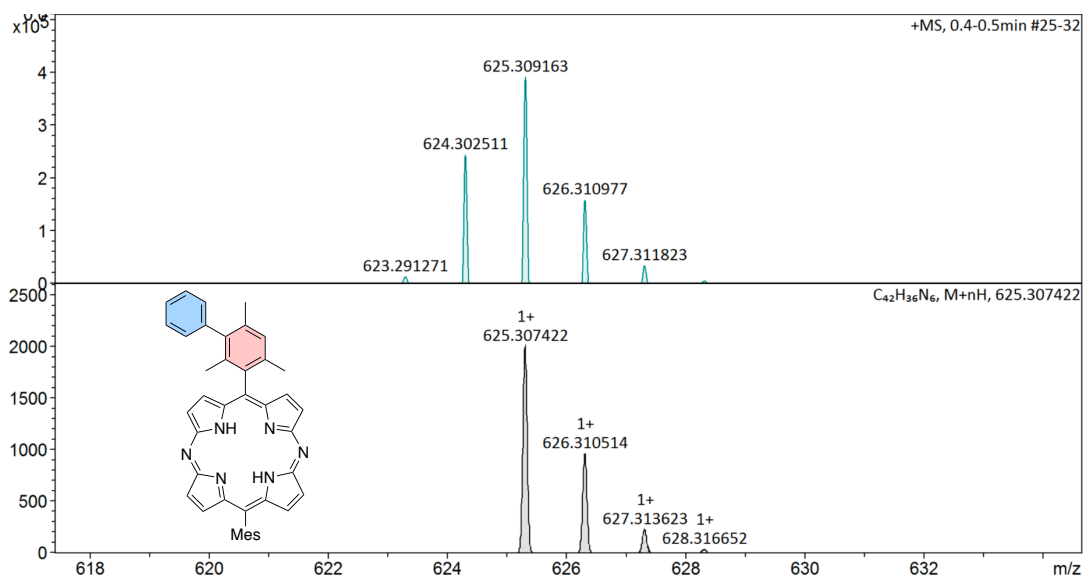


Figure S19. APCI-TOF-MS spectrum of 7.

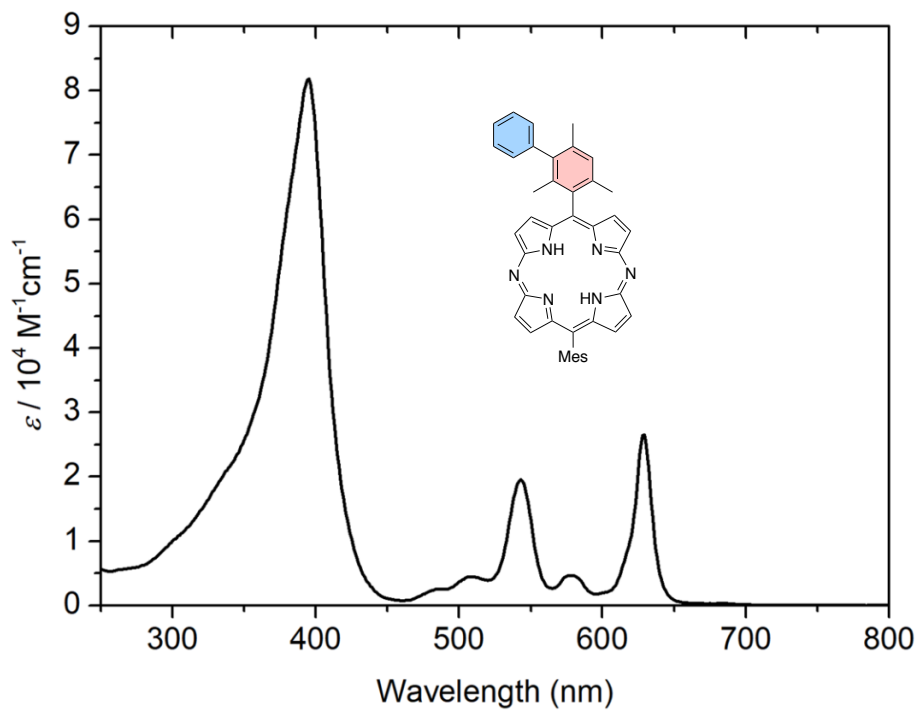


Figure S20. UV-Vis spectrum of 7 in CH_2Cl_2 .

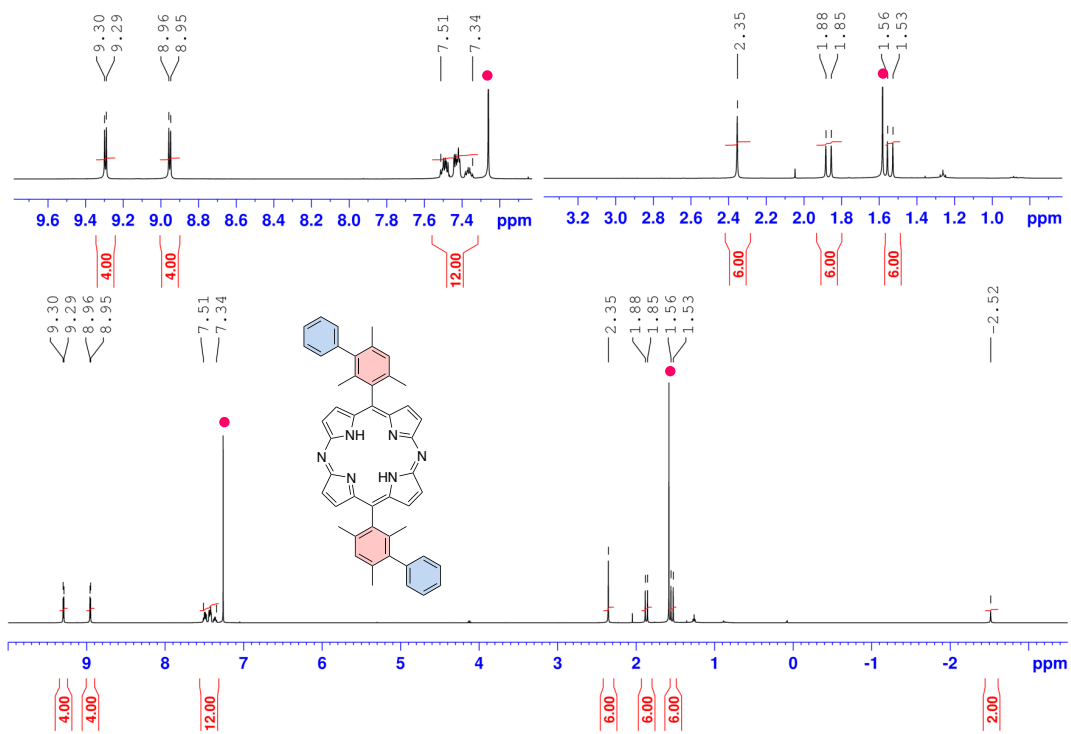


Figure S21. ^1H NMR spectrum of **8a** in CDCl_3 .

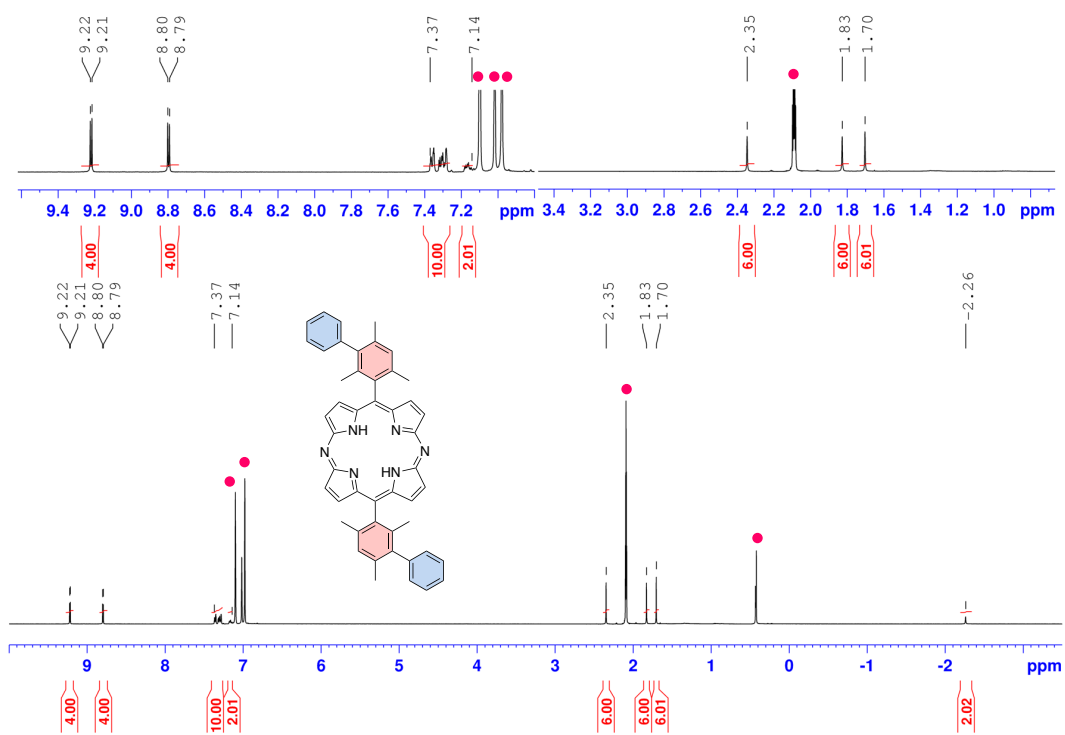


Figure S22. ^1H NMR spectrum of **8a** in $\text{toluene-}d_8$.

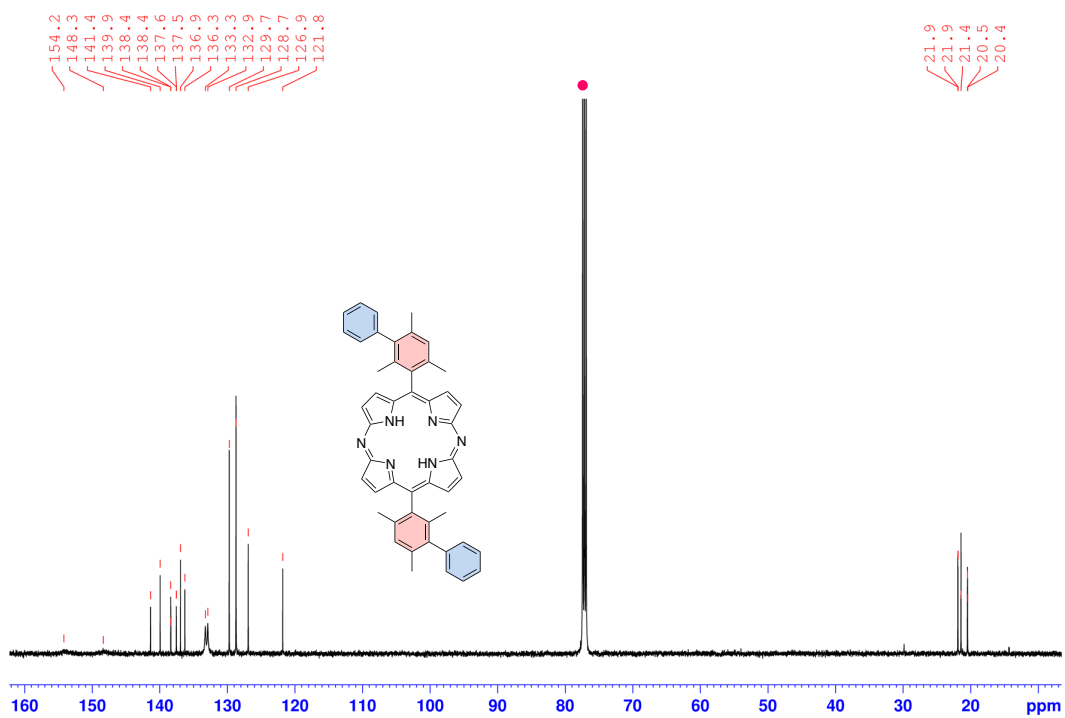


Figure S23. $^{13}\text{C}\{^1\text{H}\}$ NMR spectrum of **8a** in CDCl_3 .

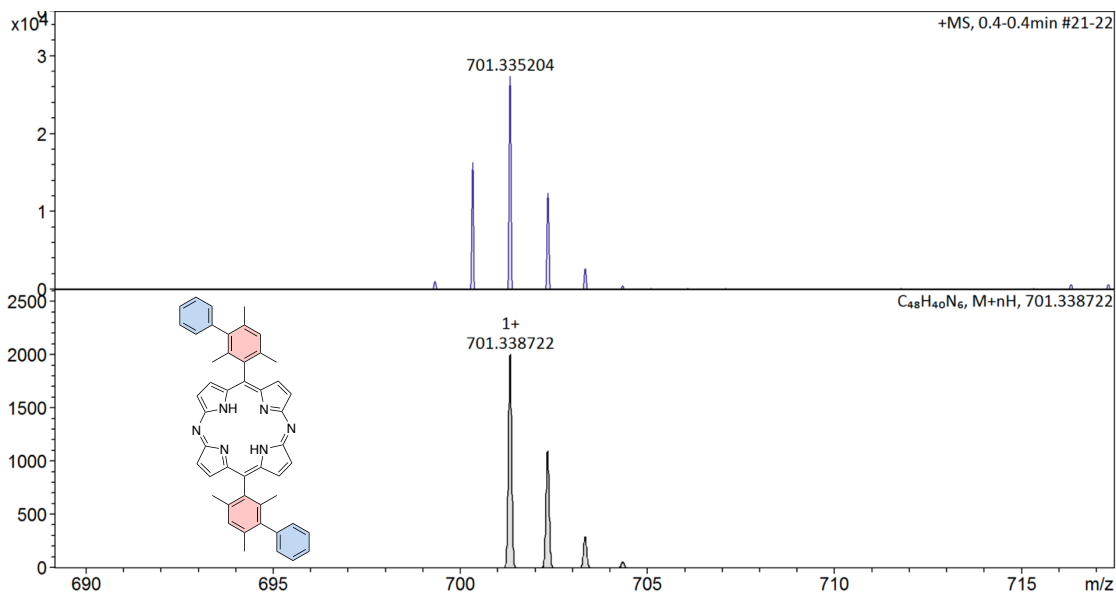


Figure S24. APCI-TOF-MS spectrum of **8a**.

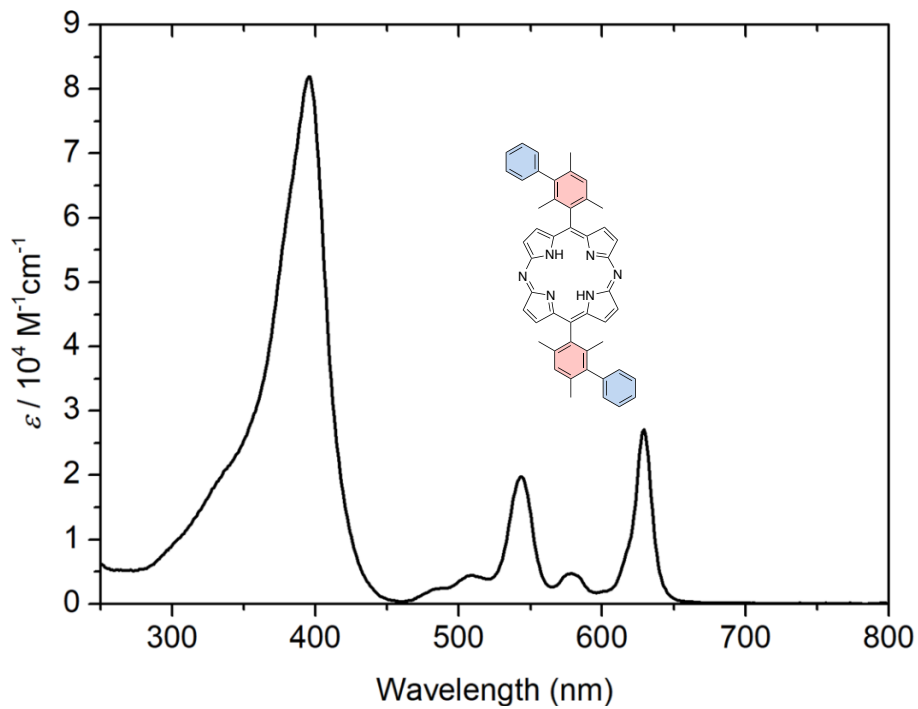


Figure S25. UV-Vis spectrum of **8a** in CH_2Cl_2 .

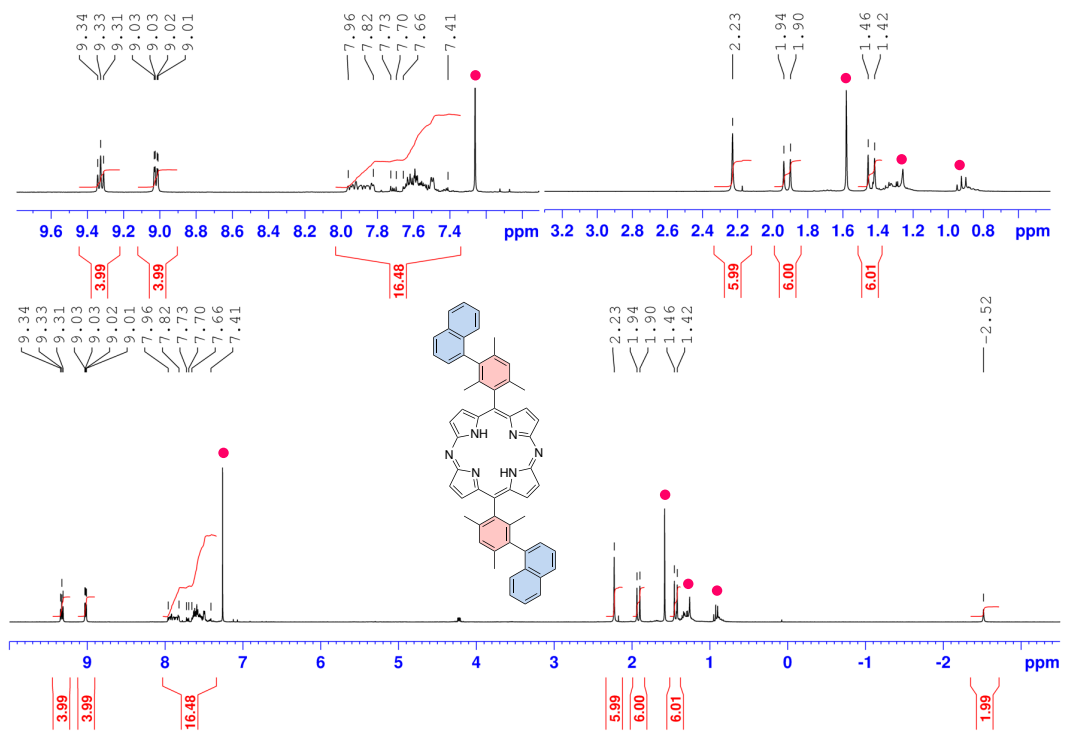


Figure S26. ^1H NMR spectrum of **8b** in CDCl_3 .

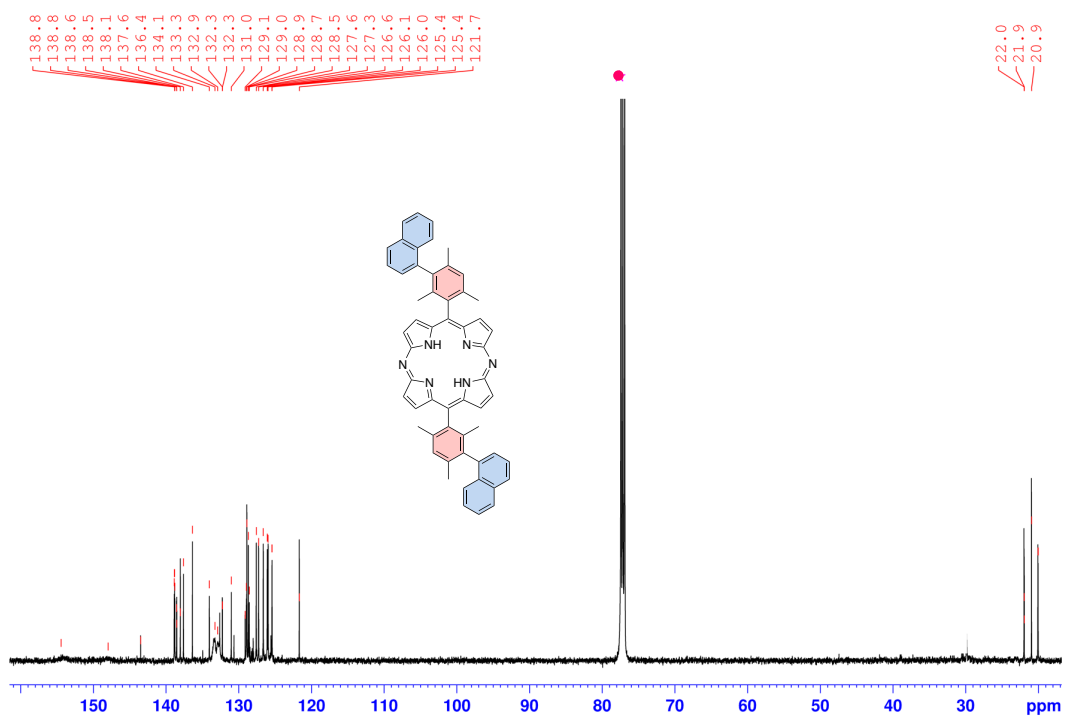


Figure S27. $^{13}\text{C}\{^1\text{H}\}$ NMR spectrum of **8b** in CDCl_3 .

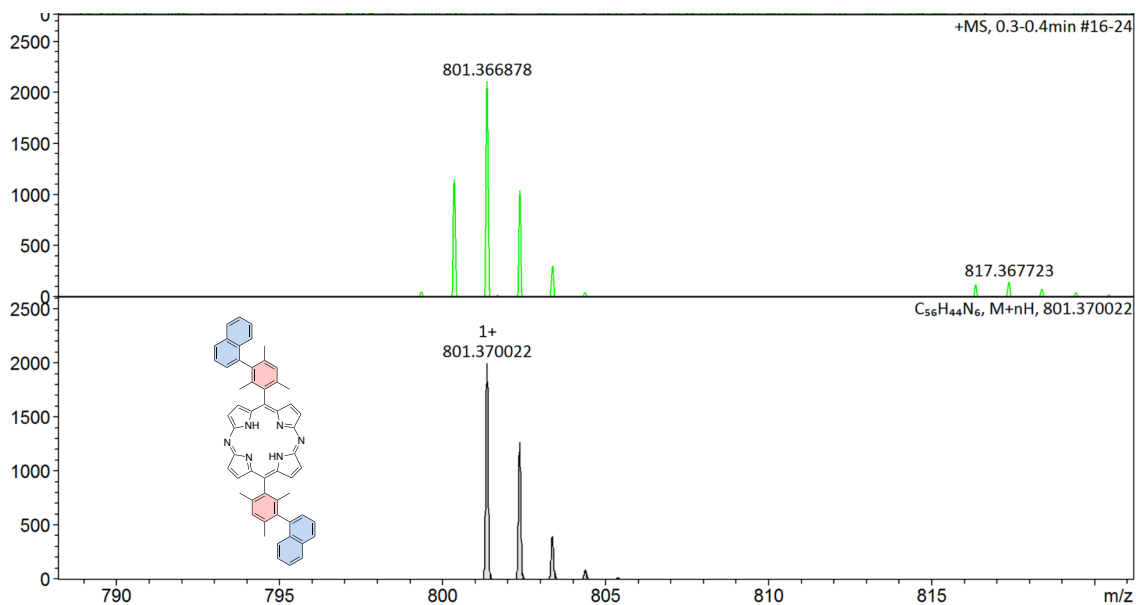


Figure S28. APCI-TOF-MS spectrum of **8b**.

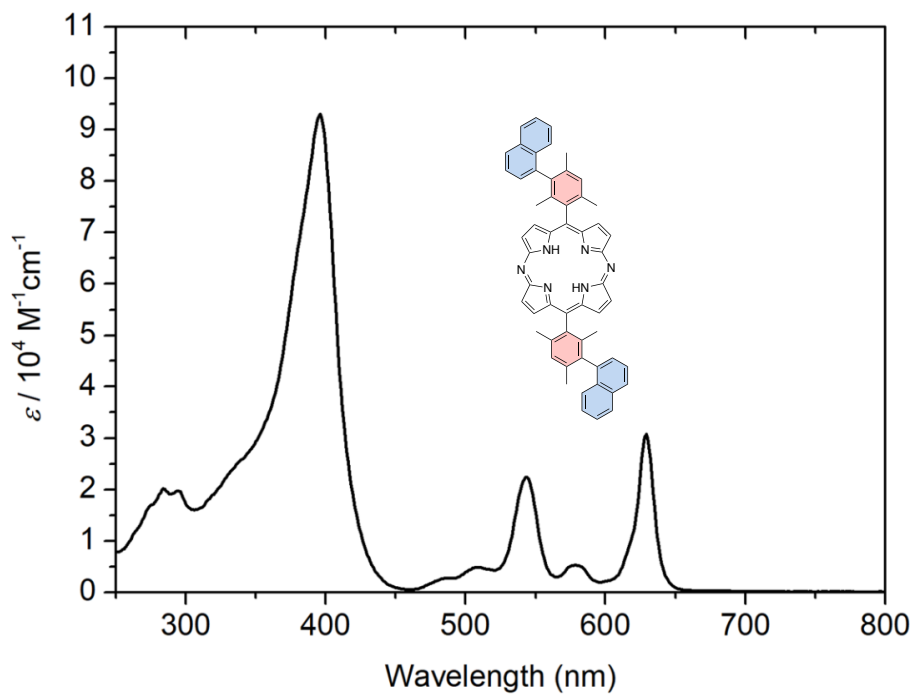


Figure S29. UV-Vis spectrum of **8b** in CH_2Cl_2 .

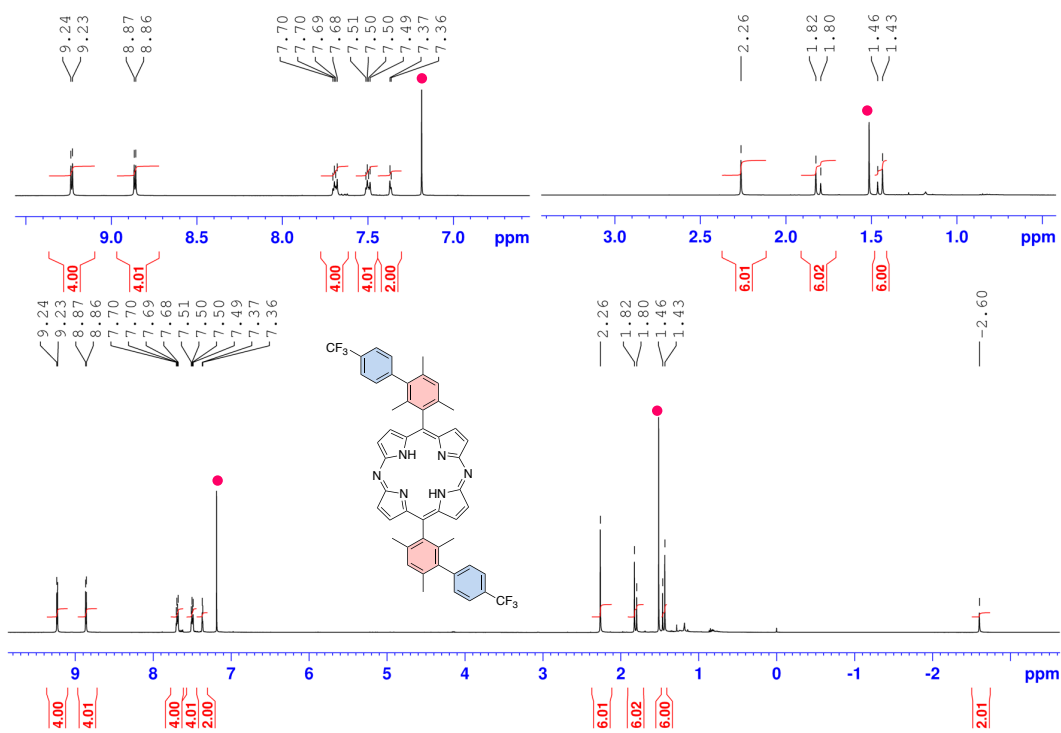


Figure S30. ^1H NMR spectrum of **8c** in CDCl_3 .

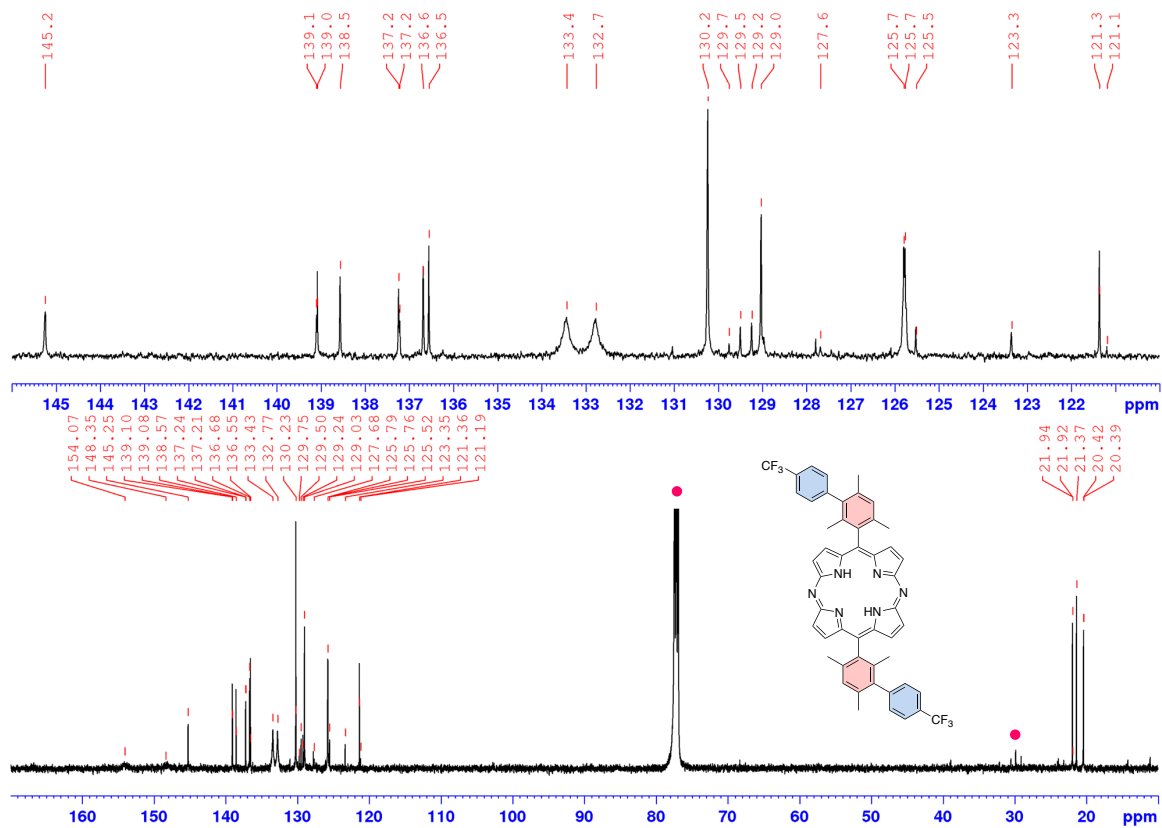


Figure S31. $^{13}\text{C}\{^1\text{H}\}$ NMR spectrum of **8c** in CDCl_3 .

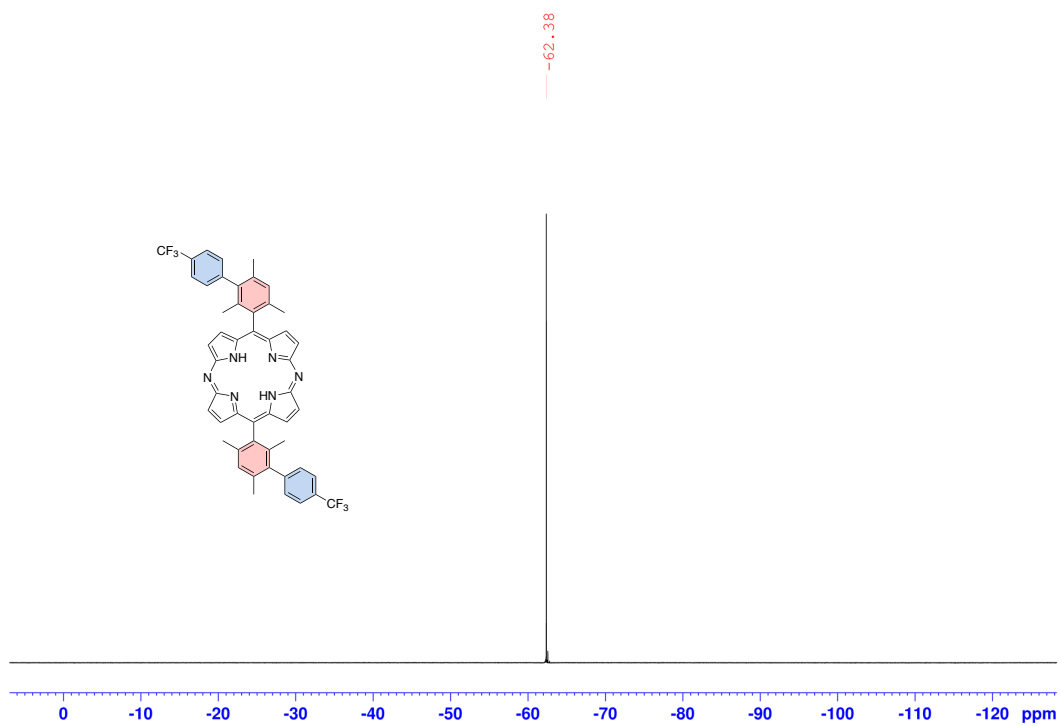


Figure S32. ^{19}F $\{^1\text{H}\}$ NMR spectrum of **8c** in CDCl_3 .

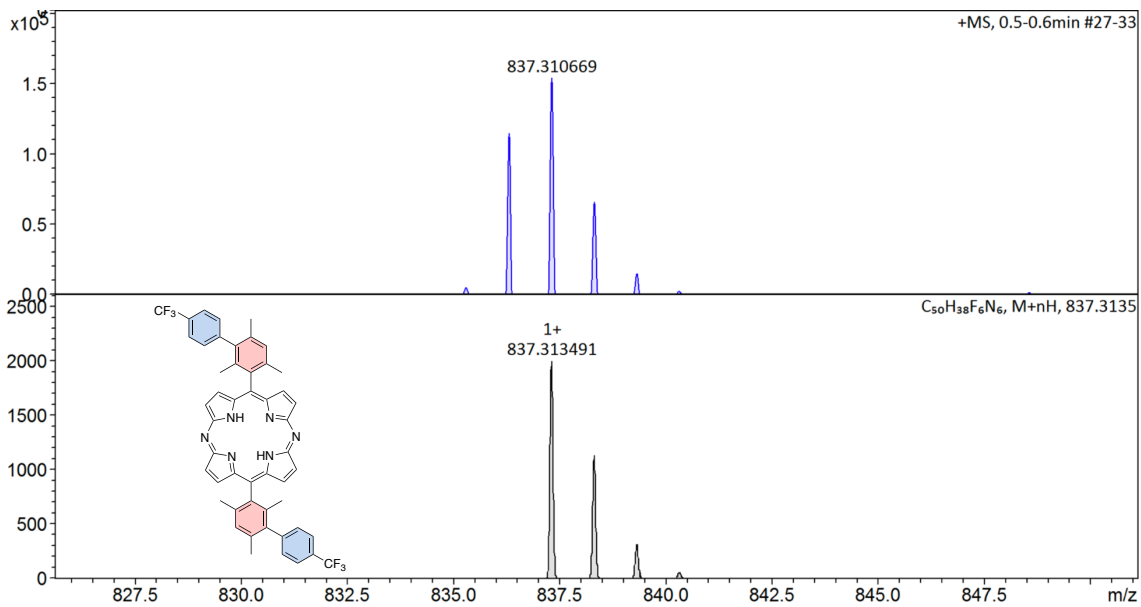


Figure S33. APCI-TOF-MS spectrum of **8c**.

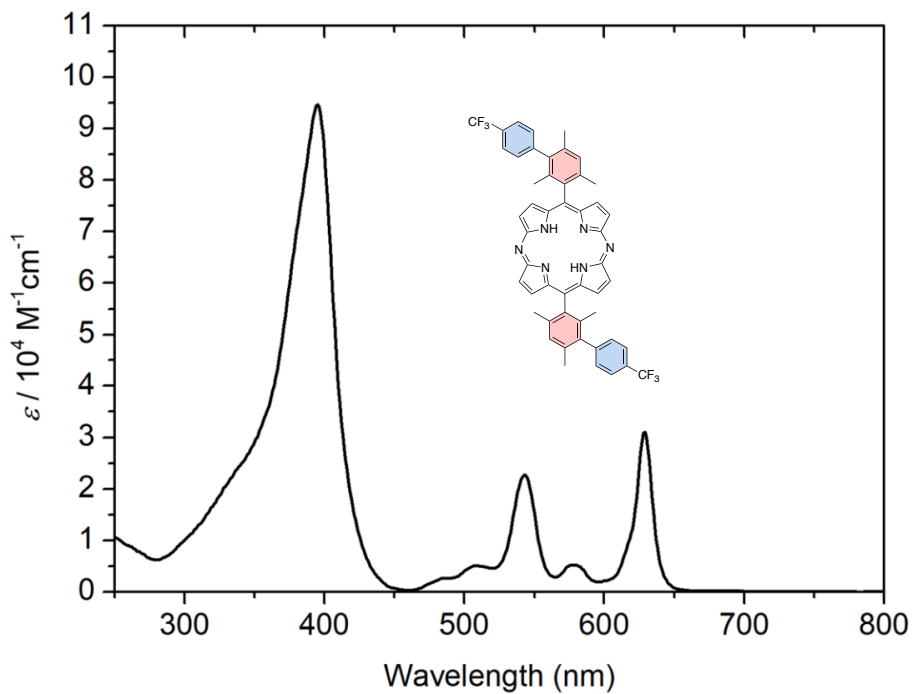


Figure S34. UV-Vis spectrum of **8c** in CH_2Cl_2 .

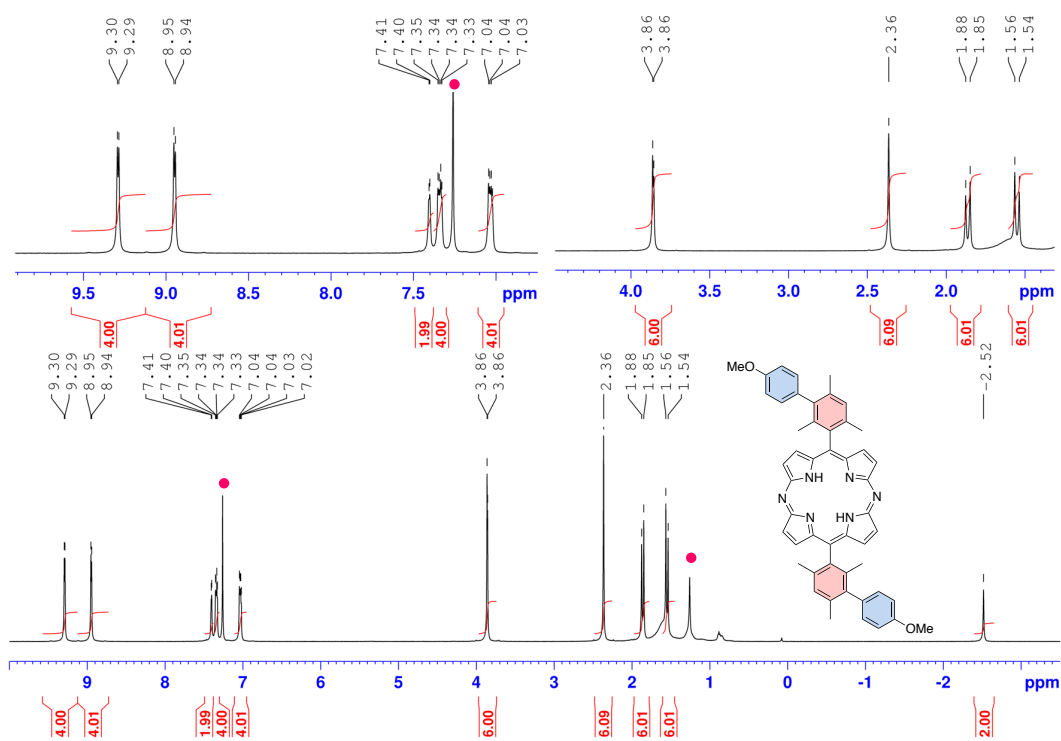


Figure S35. ¹H NMR spectrum of **8d** in CDCl₃.

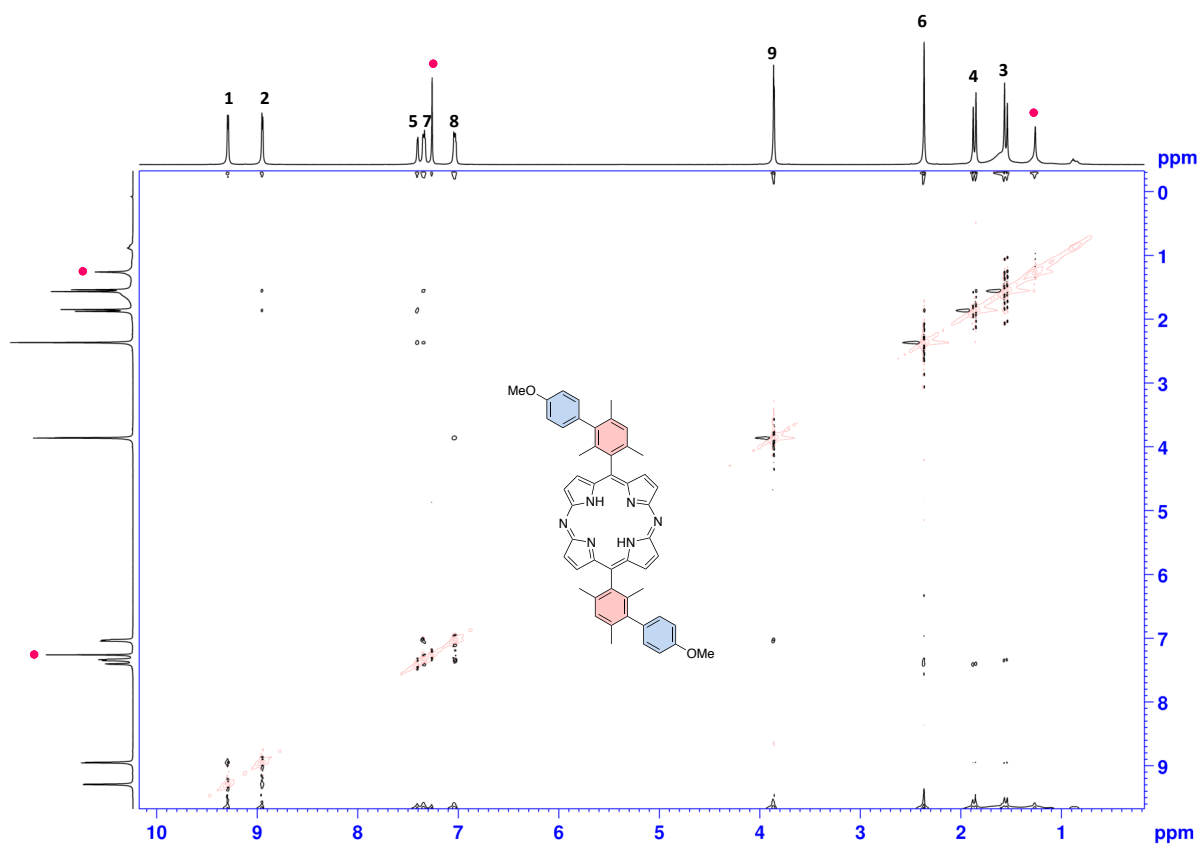


Figure S36. ROESY spectrum of **8d** in CDCl₃.

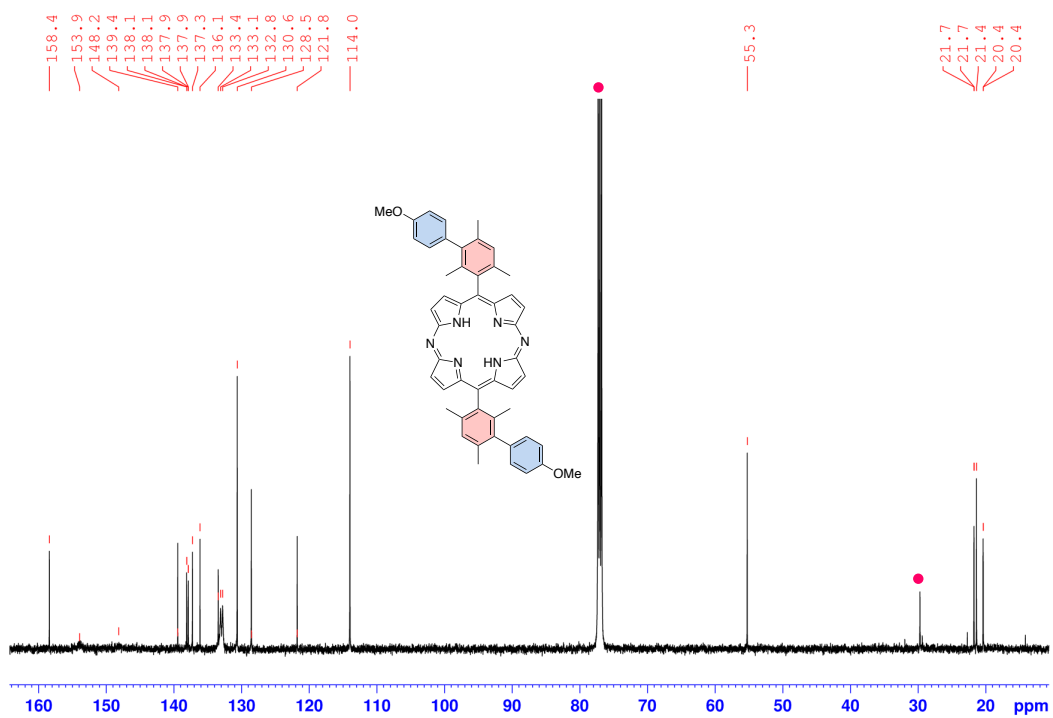


Figure S37. $^{13}\text{C}\{^1\text{H}\}$ NMR spectrum of **8d** in CDCl_3 .

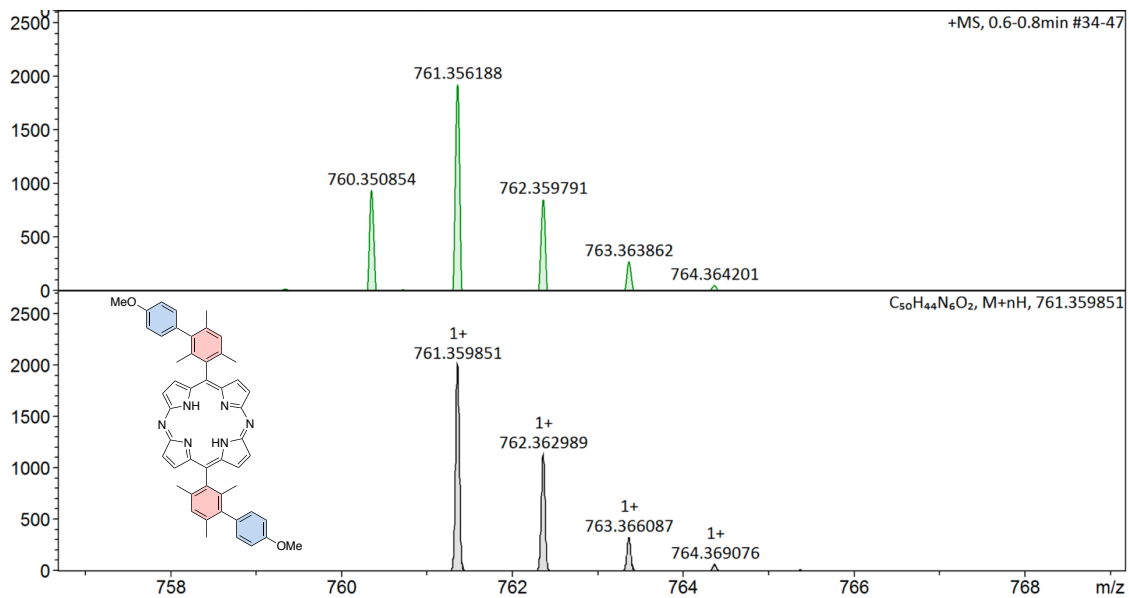


Figure S38. APCI-TOF-MS spectrum of **8d**.

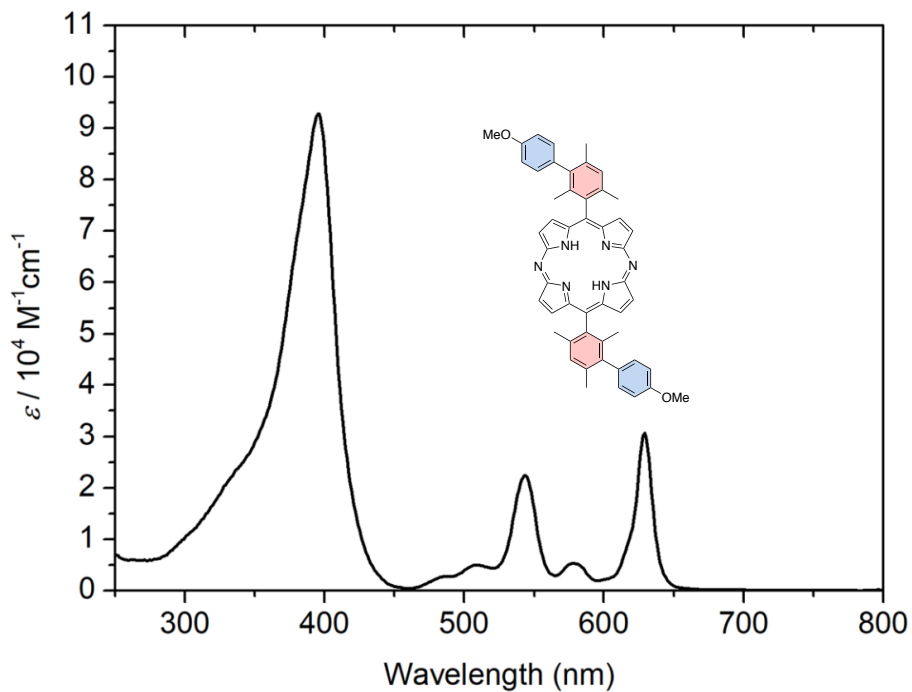


Figure S39. UV-Vis spectrum of **8d** in CH_2Cl_2 .

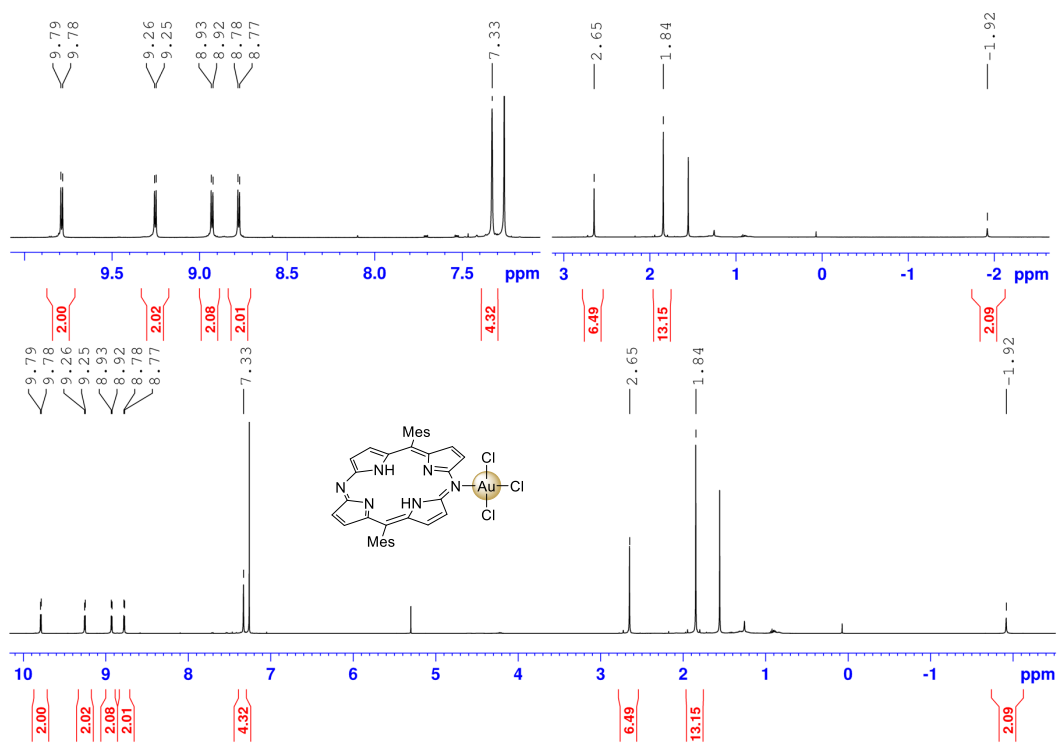


Figure S40. ^1H NMR spectrum of **9** in CDCl_3 .

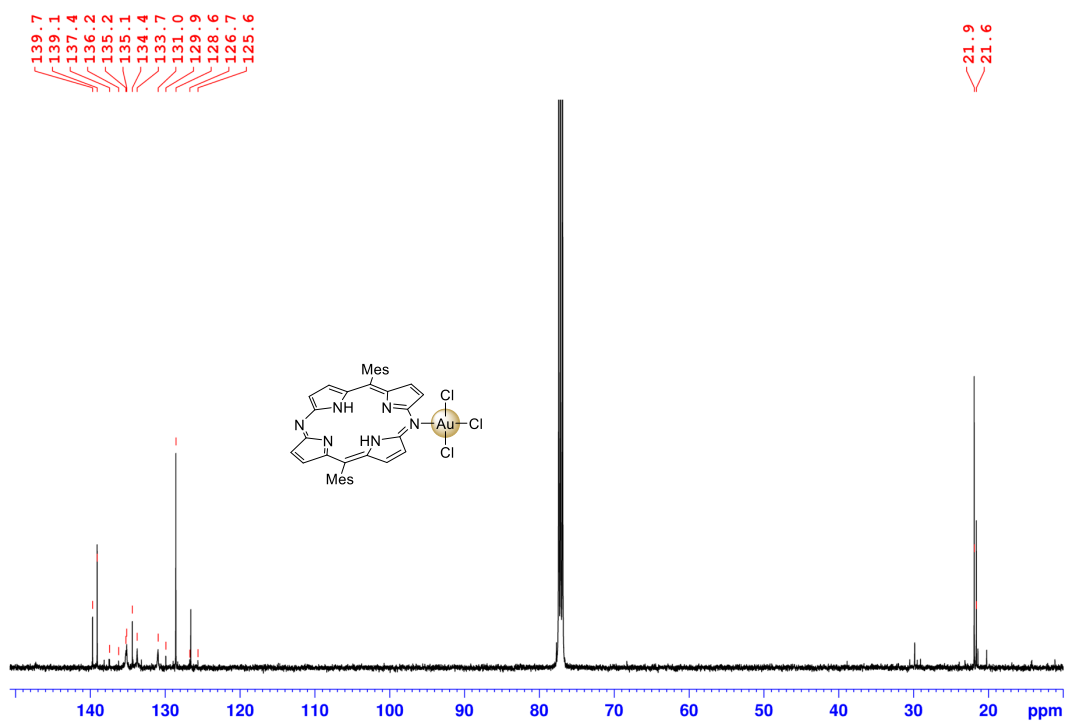


Figure S41. $^{13}\text{C}\{^1\text{H}\}$ NMR spectrum of **9** in CDCl_3 .

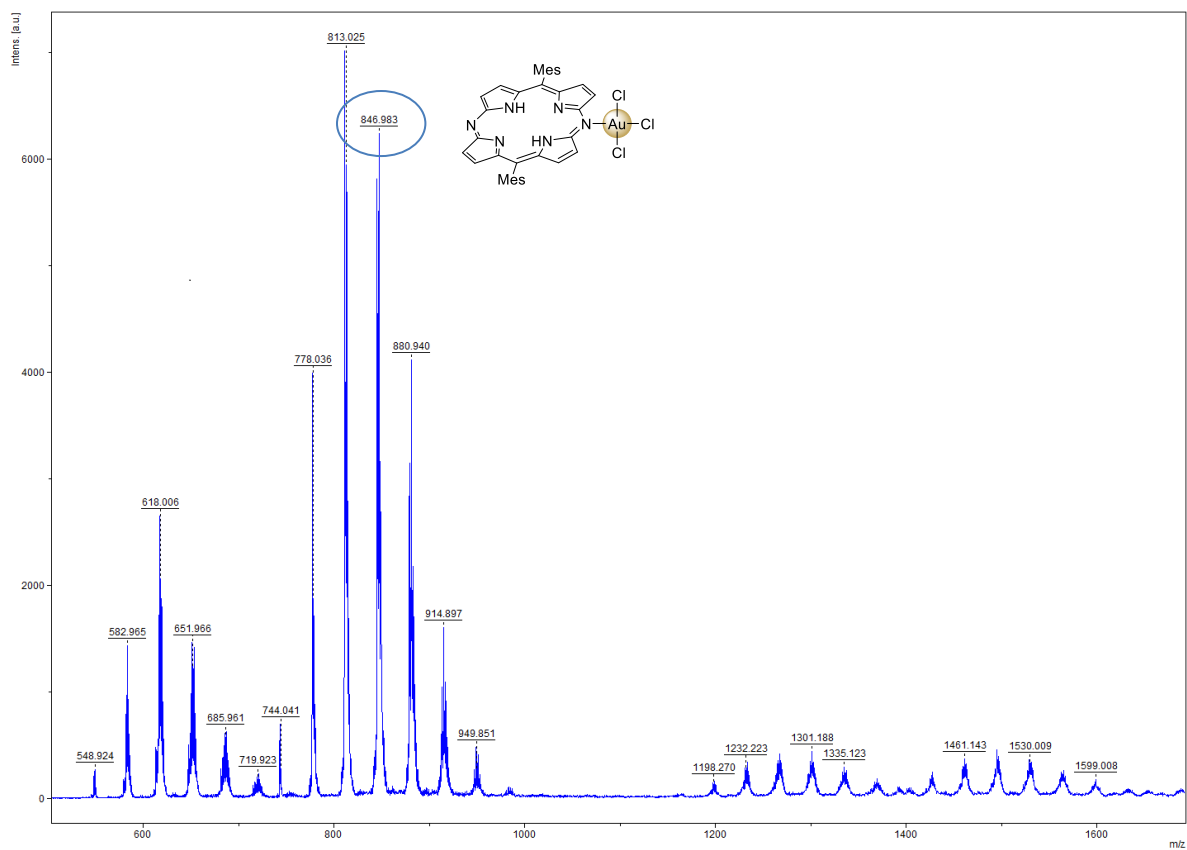


Figure S42. MALDI-TOF-MS spectrum of **9**.

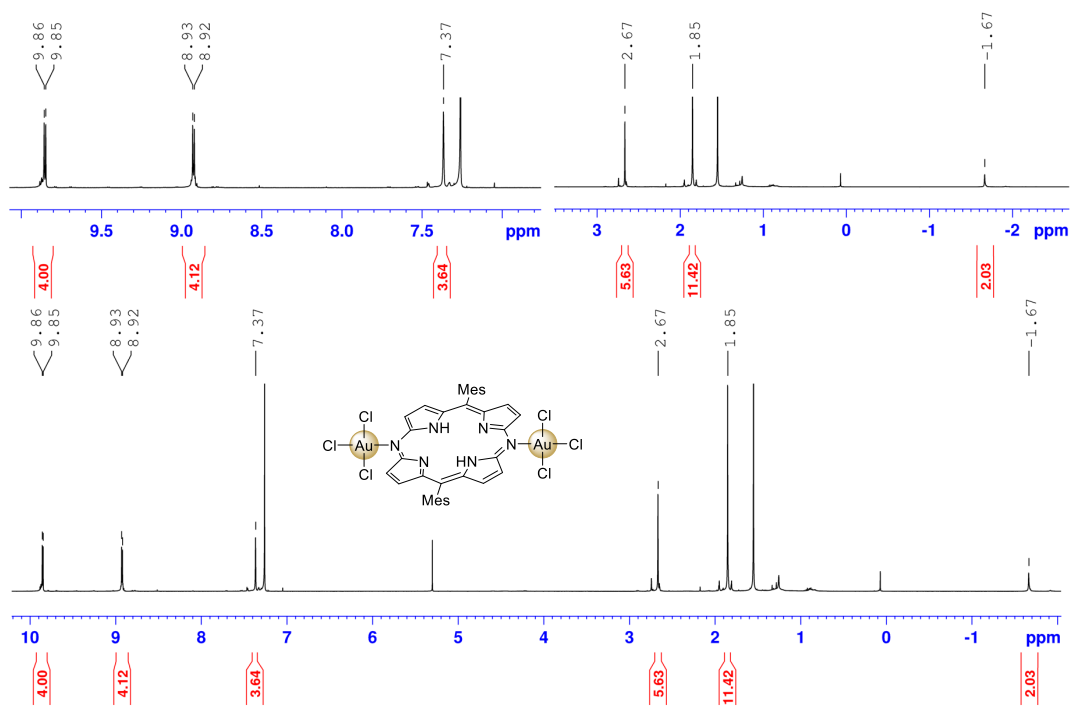


Figure S43. ¹H NMR spectrum of **10** in CDCl₃.

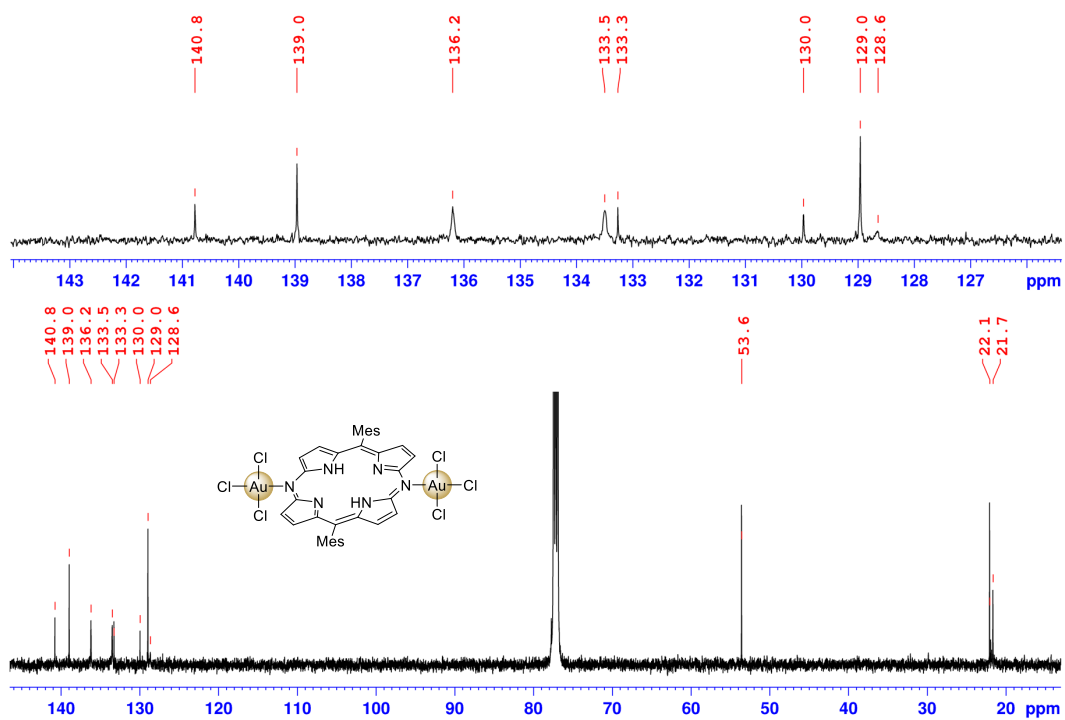


Figure S44. $^{13}\text{C}\{^1\text{H}\}$ NMR spectrum of **10** in CDCl_3 .

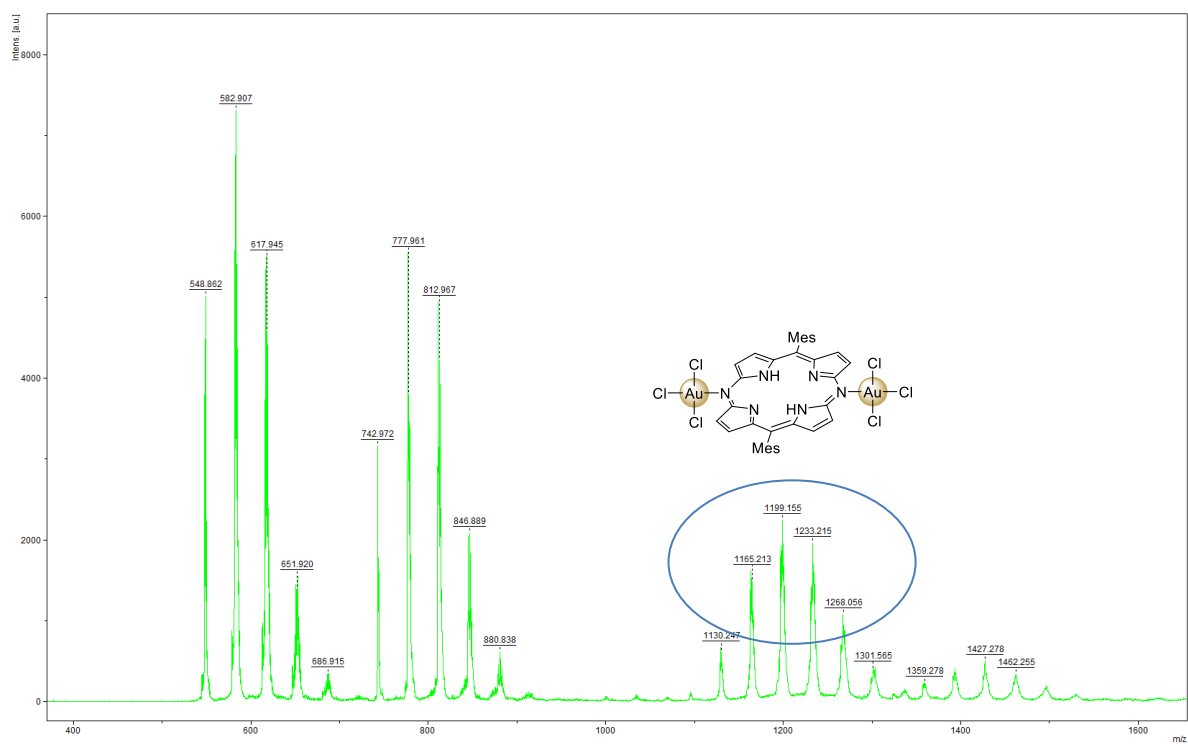


Figure S45. MALDI-TOF-MS spectrum of **10**.

X-ray Diffraction Analysis

X-ray data of **3H-Cl**, **9** and **10** were taken on a Rigaku CCD diffractometer (Saturn 724 with MicroMax-007) with Varimax Mo optics using graphite monochromated Mo-K α radiation ($\lambda = 0.71075$ Å). Crystallographic data for **3H-Cl**, **9** and **10** have been deposited with the Cambridge Crystallographic Data Centre as supplementary publication no. CCDC-2014575, 2031076, and 2032240, respectively.

Table S1. Crystal data and structure refinements for **3H-Cl**, **9** and **10**.

Compound	3H-Cl	9	10
Empirical Formula	C ₁₈ H ₁₄ ClN ₃	C _{18.5} H _{16.5} Au _{0.5} Cl ₃ N ₃	C _{18.5} H _{16.5} AuCl _{4.5} N ₃
<i>M_w</i>	307.77	485.68	637.34
Crystal System	monoclinic	monoclinic	monoclinic
Space Group	<i>P</i> 2 ₁ / <i>a</i> (No. 14)	<i>C</i> 2/ <i>c</i> (No. 15)	<i>P</i> 2 ₁ / <i>a</i> (No. 14)
<i>a</i>	7.8431(6) Å	26.5741(6) Å	14.5210(7) Å
<i>b</i>	23.827(2) Å	11.7909(2) Å	10.7731(5) Å
<i>c</i>	8.7706(7) Å	12.2513(3) Å	13.0542(5) Å
β	114.206(9)°	90.465(2)°	93.566(4)°
Volume	1494.9(2) Å ³	3838.60(14) Å ³	2038.20(16) Å ³
<i>Z</i>	4	8	4
Density (calcd.)	1.367 g/cm ³	1.681 g/cm ³	2.077 g/cm ³
Goodness-of-Fit	1.173	1.081	1.077
<i>R</i> ₁ [<i>I</i> > 2 σ (<i>I</i>)]	0.1135	0.0654	0.0608
<i>wR</i> ₂ (all data)	0.2151	0.1942	0.1594
Temperature [K]	93(2)	93(2)	93(2)

Electrochemical Analysis

Cyclic voltammograms and differential pulse voltammograms of **1H**, **7**, **8a**, **8b**, **8c**, and **8d** were recorded using an ALS electrochemical analyzer 612C. Measurements were performed in freshly distilled CH_2Cl_2 with tetrabutylammonium hexafluorophosphate as the electrolyte. A three-electrode system was used. The system consisted of a platinum working electrode, a platinum wire, and Ag/AgNO_3 as the reference electrode. The scan rate was 100 mVs^{-1} . The measurement was performed under nitrogen atmosphere. All potentials are referenced to the potential of ferrocene/ferrocenium cation couple.

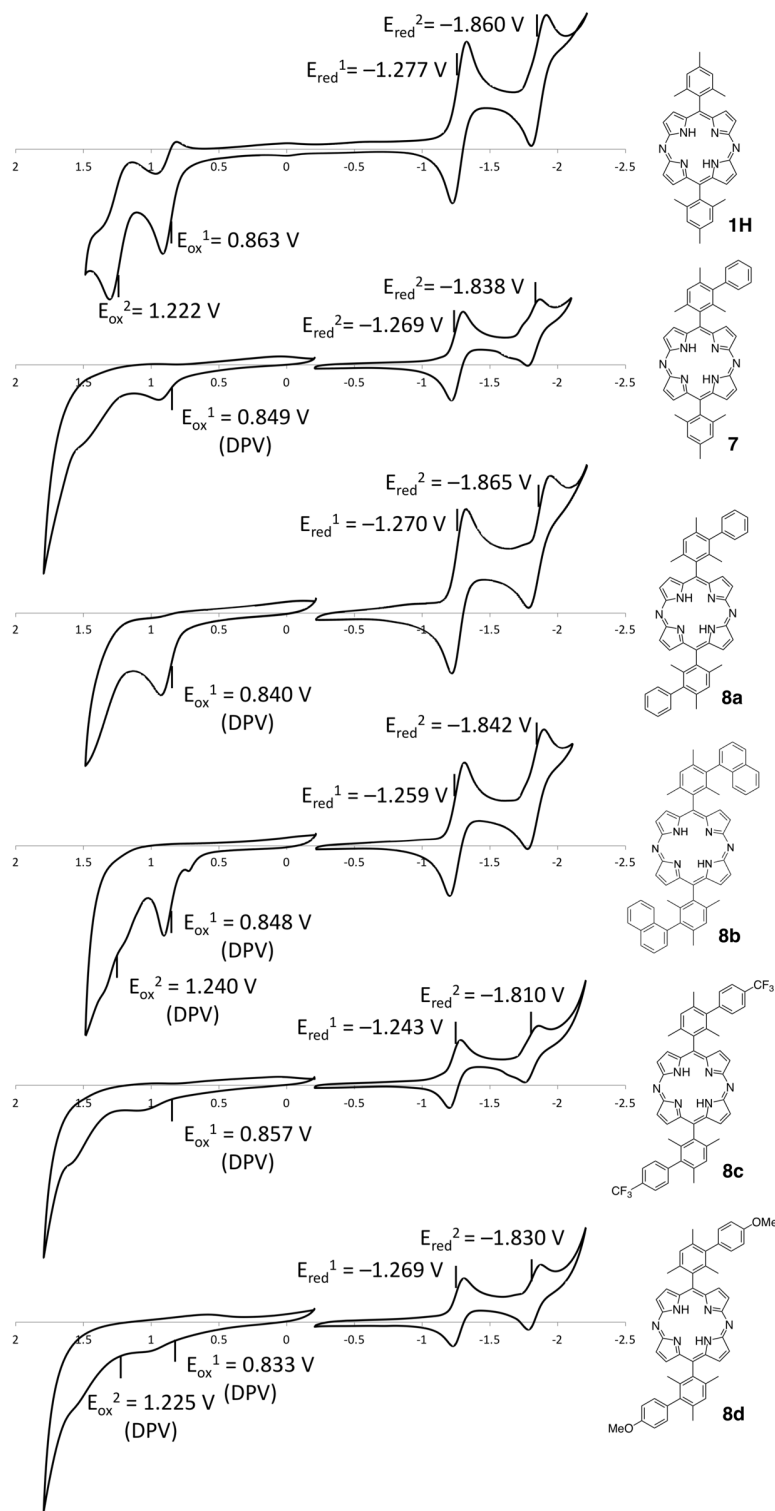


Figure S46. Cyclic voltammograms of **1H**, **7**, **8a**, **8b**, **8c**, and **8d** in CH_2Cl_2 .

Theoretical Calculations

All calculations were performed using the Gaussian 09 program.² All the structures were fully optimized without any symmetry restriction at the Becke's three-parameter hybrid exchange functional and the Lee–Yang–Parr correlation functional (B3LYP)³ and a basis set consisting of SDD⁴ for Ni and 6-31G(d) for the rest.

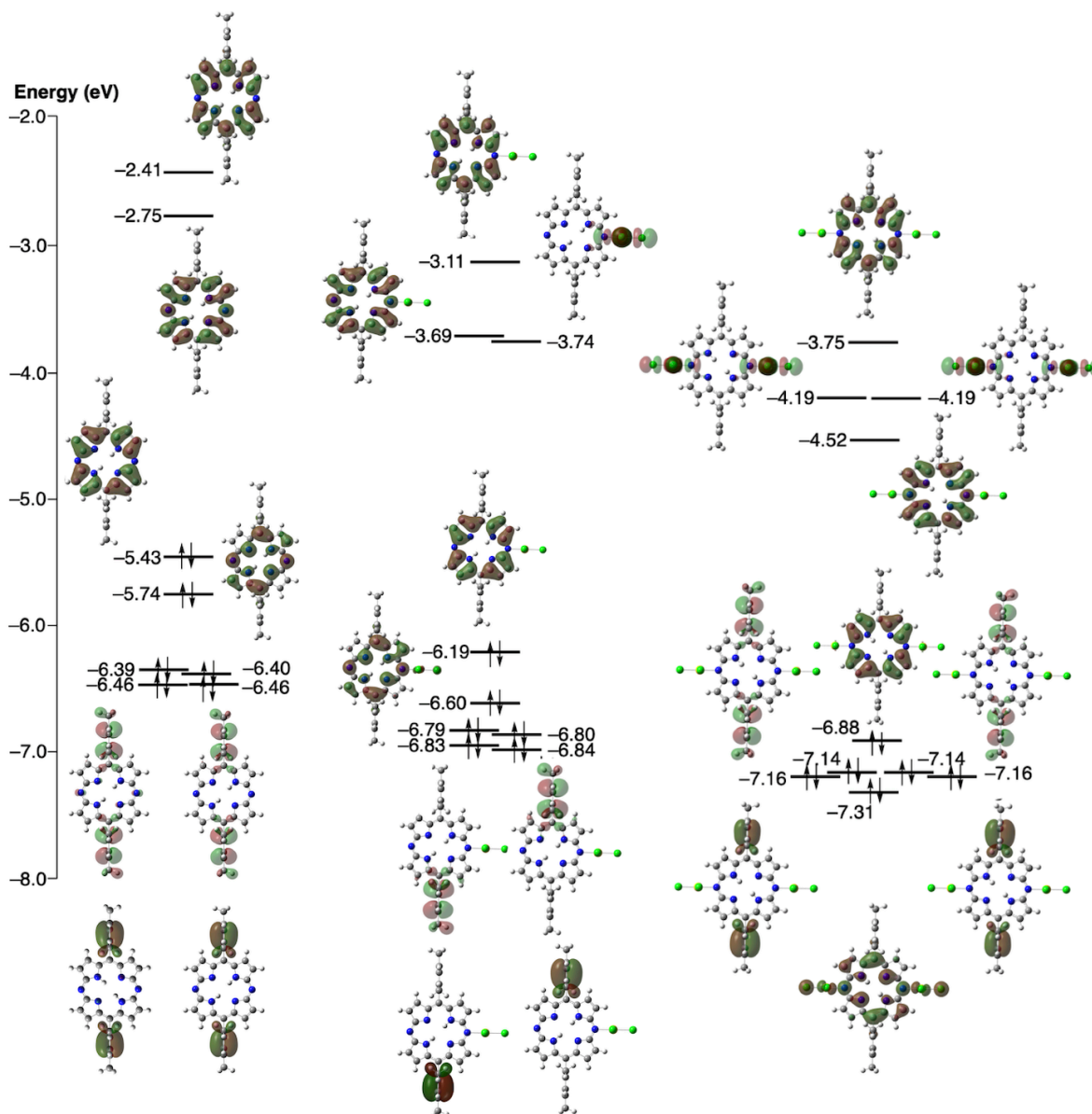


Figure S47. Molecular orbital diagrams of **1**, **9**, and **10** calculated the B3LYP/6-31G(d)+SDD level.

References

- 1) Matano, Y.; Shibano, T.; Nakano, H.; Kimura, Y.; Imahori, H. *Inorg. Chem.* **2012**, *51*, 12879–12890.
- 2) Gaussian 09, Revision D.01, Frisch, M. J.; Trucks, G. W.; Schlegel, H. B.; Scuseria, G. E.; Robb, M. A.; Cheeseman, J. R.; Scalmani, G.; Barone, V.; Mennucci, B.; Petersson, G. A.; Nakatsuji, H.; Caricato, M.; Li, X.; Hratchian, H. P.; Izmaylov, A. F.; Bloino, J.; Zheng, G.; Sonnenberg, J. L.; Hada, M.; Ehara, M.; Toyota, K.; Fukuda, R.; Hasegawa, J.; Ishida, M.; Nakajima, T.; Honda, Y.; Kitao, O.; Nakai, H.; Vreven, T.; Montgomery, Jr., J. A.; Peralta, J. E.; Ogliaro, F.; Bearpark, M.; Heyd, J. J.; Brothers, E.; Kudin, K. N.; Staroverov, V. N.; Kobayashi, R.; Normand, J.; Raghavachari, K.; Rendell, A.; Burant, J. C.; Iyengar, S. S.; Tomasi, J.; Cossi, M.; Rega, N.; Millam, J. M.; Klene, M.; Knox, J. E.; Cross, J. B.; Bakken, V.; Adamo, C.; Jaramillo, J.; Gomperts, R.; Stratmann, R. E.; Yazyev, O.; Austin, A. J.; Cammi, R.; Pomelli, C.; Ochterski, J. W.; Martin, R. L.; Morokuma, K.; Zakrzewski, V. G.; Voth, G. A.; Salvador, P.; Dannenberg, J. J.; Dapprich, S.; Daniels, A. D.; Farkas, Ö.; Foresman, J. B.; Ortiz, J. V.; Cioslowski, J.; Fox, D. J. Gaussian, Inc., Wallingford CT, 2009.
- 3) (a) Becke, A. D. *Phys. Rev. A* **1988**, *38*, 3098. (b) Lee, C.; Yang, W.; Parr, R. G. *Phys. Rev. B* **1988**, *37*, 785.
- 4) Dolg, M.; Wedig, U.; Stoll, H.; Preuss, H. *J. Chem. Phys.* **1987**, *86*, 866.